

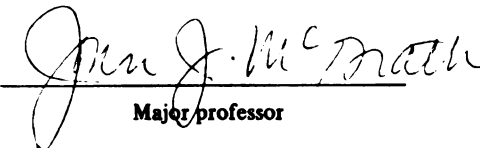
This is to certify that the
thesis entitled

"An Analytical Study of
the Convection Stage of a Cryomicroscope System"
presented by

Hasmukhbhai Patel

has been accepted towards fulfillment
of the requirements for

Master's degree in Mechanical Engineering


Major professor

Date 11/11/81



RETURNING MATERIALS:
Place in book drop to
remove this checkout from
your record. FINES will
be charged if book is
returned after the date
stamped below.

SEP 17 2001

AN ANALYTICAL STUDY OF THE CONVECTION STAGE
OF A CRYOMICROSCOPE SYSTEM

By

HASMUKHBHAI K. PATEL

A THESIS

Submitted to
Michigan State University
in partial fulfillment of the requirements
for the degree of

MASTER OF SCIENCE

Department of Mechanical Engineering

1981

ABSTRACT

AN ANALYTICAL STUDY OF THE CONVECTION STAGE OF A CRYOMICROSCOPE SYSTEM

By

Hasmukhbhai K. Patel

The present study describes a numerical analysis of the hydrodynamic and thermal characteristics of a heat transfer system designed to produce thermal control of a small sample placed on a light microscope.

A simplified model of an actual system has been developed. The model consists of a laminar flow in a rectangular duct of aspect ratio 0.3. The velocity field in the hydrodynamically fully developed region is solved. This solution is used in the thermally developing region where the duct experiences uniform heat flux at the top (heater) surface and is insulated on the other three sides.

The numerical solutions have been obtained using the finite difference technique with the Gauss-Siedel method (using successive over relaxation) and the Alternative Direction Implicit Method.

The temperature field on the surface of the heater (the site of the biological specimen) is presented and it reveals unacceptably severe temperature gradients in both the axial and lateral directions ($280^{\circ}\text{C}/\text{CM}$ and $320^{\circ}\text{C}/\text{CM}$

respectively). These results are in qualitative agreement with experimental data obtained from the actual system.

Results for the velocity field indicate that the solution yields accurate results based on mean velocity criteria (U_{mean}) but may be inaccurate by as much as 20% based on local velocity gradient criteria (C_f). Thus the results for the temperature field on the heater surface may be in error by a comparable magnitude even though an energy balance based on mean temperatures is accurate to less than 1%.

Modifications in the computer program required for model improvement and further recommendations for thermal design studies are discussed.

Dedicated to my dear Brother and my friend
Chunibhai and Hirokiyoda
without whose support and encouragement
this work would never have been completed.

ACKNOWLEDGMENT

The author is deeply indebted to Professor J. McGrath for his efforts, guidance, encouragement and patience.

The author avails this opportunity to thank all the faculty members of the Mechanical Engineering Department, Michigan State University, East Lansing.

The author wishes to express appreciation to Professor J. V. Beck, Professor J. F. Foss and the Honorable Chairman Professor John Brighton for their timely assistance on many occasions in spite of their heavy engagements.

Also the author wishes to express appreciation to Mr. Kim Hull for his technical assistance and help, and Mr. Narendra Dahotre for his help and encouragement.

TABLE OF CONTENTS

LIST OF TABLES	vi
LIST OF FIGURES	vii
NOMENCLATUREviii

Chapter

1.	INTRODUCTION	1
	1.1 Background	1
	1.2 The Actual Cryomicroscope System	2
	1.3 Fluid Mechanics and Heat Transfer Aspects of the Actual System Compared to the Model System	4
	1.4 Previous Solutions Available	6
	1.5 Specification of Model Duct and Heater Based Upon a Proposed Experimental System	7
	1.6 The Model Duct/Heater System	7
2.	HYDRODYNAMIC CONSIDERATIONS	14
	2.1 Non-Dimensionalized and Finite Differ- ence Momentum Equations With Specific Boundary Conditions	14
	2.2 Hydrodynamic Solution of the Problem	17
	2.3 Conclusions and Comments on the Hydro- dynamic Solution	27
3.	THERMAL CONSIDERATIONS	33
	3.1 Dimensional Approach for the Thermal Solution of the Problem	33
	3.2 Thermal Problem Solution by the Finite Difference Approach	40
	3.3 Conclusions and Comments on the Thermal Solution	53

Chapter

4.	DISCUSSION AND CONCLUSIONS	63
	4.1 Discussion and Conclusions	63
	4.2 Suggestions for Future Work	64
	APPENDIX A: Methods of Iteration	67
	APPENDIX B: ADI Method	74
	APPENDIX C: Tridiagonal Matrix Algorithm .	77
	APPENDIX D: Program 'HEAT'	79
	APPENDIX E: Convection Program	80
	APPENDIX F: Non-Dimensionalization of Momentum Equation for Fully Developed Flow	86
	REFERENCES	90

LIST OF TABLES

Table

1	Non-Dimensional Velocities $U^+(y^+, z^+)$ as a Function of Non-Dimensional Position .	21
2	Velocities $U(y, z)$ in (m/sec)	21
3	Temperatures at Different Locations in the Rectangular Duct at Various Distances from the Leading Edge of the Heater	44
4	Temperature of the Heater Centerline as a Function of Distance from the Leading Edge of the Heater	50
5	Results by Cess and Shaffer Method	61

LIST OF FIGURES

Figure		
1	Schematic Diagram of Cryomicroscopic System .	3
2	Temperature Gradients in Original Cryomicro- scopic system	5
3	Developing and Developed (Hydrodynamically) Regions	10
4	Reynolds Number and Mass Flow Rate as a Function of Total Pressure Drop	12
5	Finite Difference Control Volume	16
6	Non-Dimensional Hydrodynamic Boundary Condi- tions on Rectangle Cross Section Quarter . . .	19
7	Non-Dimensional Velocity and Hydrodynamic Boundary Conditions on One Quarter of the Rectangular Cross Section	23
8	Finite Difference Approximation of the Non- Dimensional Velocity Variation in Y^+ DIR ^N at $Z^+ = 3.333$	30
9	Finite Difference Approximation of the Vari- ation of Non-Dimensional Velocity in Z^+ Direction at $Y^+ = 1.0$	31
10	Thermal Boundary Conditions on Surfaces of Rectangle Duct	34
11	Finite Difference Cross Section for Thermal Solution	38
12	Velocity Assumption in Calculating Velocity on Boundary for Thermal Solution	41
13	Non-Dimensional Temperature Parameter $R(I,J)$ Used in the A D I Method for Solving the Energy Equation	43
14	The Product of Velocity and Temperature (UT) at Different Nodes in the Duct at the Trailing Edge of the Window ($x = 5$ CM)	52
15	Predicted Variation of Temperature at Window Heater Surface in 'Z' Direction at a Given 'X'	54
16	Variation of Thermocouple Temperature with Distance from Leading Edge	55

NOMENCLATURE

A	matrix containing coefficients of the unknowns
A_c	area of cross section of the duct
a	half the height of the duct
a_{ij}	coefficient of matrix A at i^{th} row and j^{th} column
B	matrix containing constant of equations
b	half the width of the duct surfaces
C_p	specific heat of compressed air ($\text{kJ/kg}^\circ\text{K}$)
C_f	fully developed friction factor in fully developed region of the duct
$C_{f \text{ app.}}$	friction factor in developing region of the duct
D_h	hydraulic diameter of the duct
g_c	specific gravity of compressed air
i	row number
j	column number
k	thermal conductivity of compressed air ($\text{W/m}^\circ\text{K}$)
L	length of the duct (m)
L_{th}	thermal length required for full development of temperature profile (m)
L^*_{th}	dimensionless thermal length required for full development of temperature profile (m)
\dot{m}	mass flow rate of the fluid (kg/sec)
Δp	total pressure drop in the duct
Δp_1	pressure drop in the developing region of the duct
Δp_2	pressure drop in the fully developed region of the duct

p	number of parts made from the height of the duct for finite difference method
q''	heat flux input (W/m^2)
Q	total heat added to the fluid
q	number of parts made from the width of the duct for finite difference method
$R(I,J)$	constant dependent on velocity, molecular thermal diffusivity at the position (I,J)
T	temperature ($^{\circ}\text{C}$)
T_m	mean bulk fluid temperature ($^{\circ}\text{C}$)
T_{b1}	bulk temperature of fluid at the exit of the window region ($^{\circ}\text{C}$)
T_{b2}	bulk temperature of fluid at the exit of the window region ($^{\circ}\text{C}$)
U	velocity at given location (m/sec)
U^+	non-dimensional velocity
U_m	mean velocity of the compressed air in the duct (m/sec)
U^*	constant depends on pressure drop for non-dimensionalization of velocity (m/sec)
U_{\max}	maximum velocity at the center of the duct (m/sec)
V^+	non-dimensional mean velocity
W_b	optimum overrelaxation factor in S. O. R. method
X	the hydrodynamic length required for full development of the velocity profile
χ	matrix containing unknowns
x	x coordinate of the cross section
x^+	non-dimensional x coordinate of the cross section
y	y coordinate of the cross section
y^+	non-dimensional y coordinate of the cross section
z	z coordinate of the duct length
z^+	non-dimensional z coordinate of the cross section

Greek Symbols

α	molecular thermal diffusivity (m^2/sec)
ρ	fluid density (kg/m^3)
μ	dynamic viscosity coefficient ($\text{p}_a \cdot \text{sec}/\text{m}^2 \text{ sec}$)
α^*	aspect ratio of the duct
$\rho(\beta)$	specific radius of the matrix of coefficients

CHAPTER I
INTRODUCTION

1.1 BACKGROUND

The cryomicroscope is a research tool which allows a researcher to directly observe freezing and thawing processes. The better systems of this type are computer-controlled and allow precise and virtually independent control over temperature and its rate of change.

The desirable characteristics of such a system include the capability to subject a specimen to a uniform temperature process $T(x,y,z,t) = T(t)$ over a rather wide dynamic range of temperature rates of change. These characteristics make it possible to identify particular events of interest with specific temperatures and/or temperature histories. For small samples, this has been possible and a single temperature measurement provides a reasonable basis for feedback control.

The present work considers a heat transfer system which has been used to study freezing damage in the micro-circulation of a hamster cheek pouch--a macroscopic specimen that was viewed through the cryomicroscope. There is experimental evidence showing that temperature gradients of approximately $100^{\circ}\text{C}/\text{cm}$ may exist in the immediate vicinity of the specimen for this type of system.

The research presented here is a first step at improving the thermal design of such systems. A simplified model of the actual system is developed and numerical solutions of the velocity and temperature fields are presented. The computer model developed here and modifications of it

can be used to optimize the thermal design of such systems in the sense of reducing temperature gradients at the site of the specimen.

The remainder of the introduction describes the actual system more completely and presents the simplifications made in modelling the system.

1.2 THE ACTUAL CRYOMICROSCOPE SYSTEM

The cryomicroscope, developed by Diller and Cravalho at the M.I.T. Cryogenic Engineering Laboratory (1), was the primary investigative tool used by Thomas Hrcanj (2) for his experimental investigation of the freezing damage in the microcirculation of a hamster cheek pouch. The cryomicroscope consists of a Zeiss Universal light microscope (see Figure 1) that incorporates a specially designed convection stage. This convection stage is placed in the optical path of the microscope between the objective and a long working distance (7 mm) condenser. The convection stage consists of a closed rectangular channel (0.118 x 0.375 x 2.69 inch) fitted with circular quartz windows (0.9" diameter, 0.010" thick) on the top and on the bottom of the channel. These windows are located at that point along the channel which intersects the microscope objective. In this case, biological specimens are placed on the top heater window for cooling. The cheek-pouch of a sedated hamster could be everted and mounted flatly over the top window. For the convection stage used by Hrcanj (2) in his research, pre-cooled gaseous

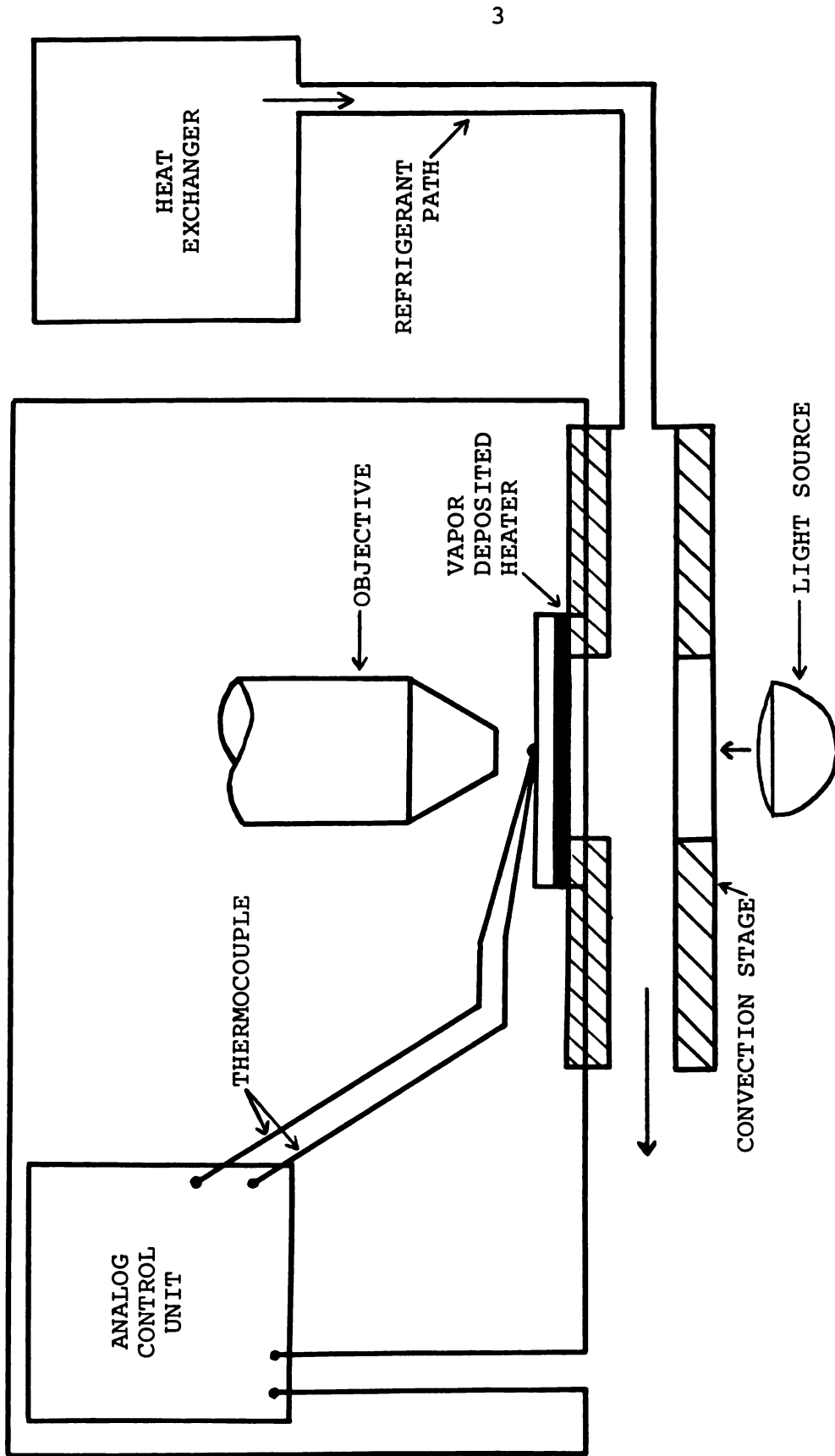


FIGURE 1. SCHEMATIC DIAGRAM OF CRYOMICROSCOPIC SYSTEM

nitrogen was convected through the closed channel. The gas stream supplied the necessary cooling capacity to freeze the cheek pouch.

The top quartz window of this system was manufactured with a thin transparent resistant film on its bottom surface. This film was therefore between the biological sample and the refrigerant fluid so that dissipation of electrical energy in the film provided thermal energy when desired to offset cooling by the refrigerant.

An analog thermal control system measured one temperature in the specimen and used this single measurement to control "the" specimen temperature by varying the heat generation in the film heater.

As shown in Figure 2, the temperature gradients in the original system could be severe. A quantitatively accurate model of this system is desired.

1.3 FLUID MECHANICS AND HEAT TRANSFER ASPECTS OF THE ACTUAL SYSTEM COMPARED TO THE MODEL SYSTEM

The actual cryomicroscope heat transfer system used by Hrcanj is characterized by several important complexities that were beyond the scope of this initial study. The following factors are included in the actual system:

- 1) flow separation at the entrance of the rectangular duct due to sudden expansion from an upstream circular tube
- 2) turbulent flow
- 3) both hydrodynamically and thermally developing flow

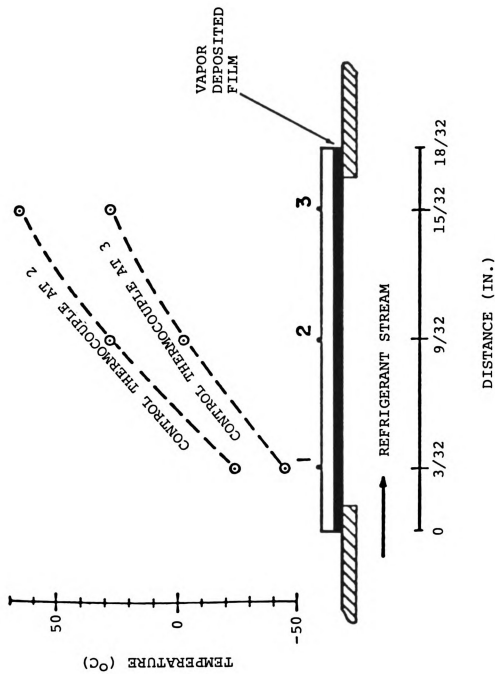


FIGURE 2. TEMPERATURE GRADIENTS IN ORIGINAL CRYOMICROSCOPIC SYSTEM

- 4) heat dissipation over circular boundary regions of the rectangular duct system
- 5) ill-defined natural convection boundary conditions over the remaining three duct surfaces

Since the present research focuses primarily on the thermal aspects of the problem, a simplified flow field was employed. Hence the flow is taken to be: (1) laminar; (2) fully developed hydrodynamically; (3) steady flow.

In addition, the thermal model primarily considers the development of the thermal boundary layer in the rectangular channel in the heater window region in order to predict quantitatively the thermal gradients on this surface. The following assumptions are made for the heat transfer calculations:

- 1) uniform heat flux from the heater window into the refrigerant fluid
- 2) adiabatic walls on the other three duct surfaces
- 3) constant fluid properties.

1.4 PREVIOUS SOLUTIONS AVAILABLE

Hornbeck (12) provides a solution to the heat transfer problem described above. However, this solution does not include the non-dimensional axial length, aspect ratio, or Reynolds number of interest here. Details of the Hornbeck technique are given later.

1.5 SPECIFICATION OF MODEL DUCT AND HEATER BASED UPON A PROPOSED EXPERIMENTAL SYSTEM

Since the model to be analyzed is not completely comparable to the actual system, the conditions to be modelled are defined in terms of a proposed experimental system which could be used to verify the numerical results obtained from the current simplified model. The conceptual experimental system serves the useful purpose of providing a specific illustration of the fluid mechanics and heat transfer concepts involved and does so on a scale that would be easily realizable in an experimental laboratory. The model fluid assumed here is compressed air since it would be readily available in most laboratories.

1.6 THE MODEL DUCT/HEATER SYSTEM

The model duct is taken to have the same cross-sectional dimensions as the original Hrycaj system (1.0 cm width by 0.3 cm height). The model heating length is arbitrarily chosen to be 5.0 cm compared to an actual length of 2.9 cm. This increased length allows prediction of temperatures for longer heaters of interest.

The simplified model assumes a completely developed hydrodynamic boundary layer in the window region with the laminar flow assumption. In order to assure the fully developed condition, the behavior of the flow was examined for a range of Reynolds numbers less than 2300, and a developing length was defined. This criteria places the model heater far enough downstream of the duct

entrance such that full development of the hydrodynamic boundary layer occurs. It has been assumed that a uniform velocity distribution would be present at the entrance of the duct.

The Reynolds number will be based upon the hydraulic diameter since this approach is found to describe flow through non-circular ducts very well (8,9). The hydraulic diameter is defined as:

$$D_h = \frac{4 \times \text{cross-sectional area}}{\text{perimeter of the cross-section}}$$

In the present case for a duct of dimensions (0.3 cm x 1.0 cm):

$$D_h = 0.4615 \text{ cm}$$

The criteria for the critical hydrodynamic development inside the duct is given by Kays and Crawford (8) in terms of the hydraulic diameter approach:

$$\frac{x}{D_h} = \frac{Re}{20}$$

Since the fluid in the duct is assumed to be air, the following property values have been used:

$$\rho = 1.1766 \text{ kg/m}^3$$

$$\mu = 18.53 \times 10^{-6} \text{ kg/m} \cdot \text{sec}$$

$$\kappa = 26.14 \times 10^{-3} \text{ W/m}^{\circ}\text{K}$$

$$C_p = 1.005 \text{ kJ/kg}^{\circ}\text{K}$$

These values are taken at 23°C and are assumed constant.

A Reynolds number of $Re_{DH} = 1827$ is arbitrarily chosen to have laminar flow and the corresponding development length is $X = 0.4215 \text{ m}$. Thus the model heater will be

placed downstream at $X = 0.475$ m and the solution will be for $Re_{DH} = 1827$ with a total duct length of 1.0 m (see Figure 3).

Although the total pressure drop in the Hrycaj system was estimated as 10-20 psig, the pressure drop required to maintain laminar flow will be considerably less than this. The pressure drop mechanism and expressions quantifying the pressure drop are different in the undeveloped and developed regions. Knowing the critical development length, we consider the two pressure drops separately and calculate the total pressure drop for the entire tube.

Let $\Delta P = \Delta P_1 + \Delta P_2 =$ total pressure drop where:

$\Delta P_1 =$ pressure drop in the developing region

$\Delta P_2 =$ pressure drop in the fully developed region

Shah and London (9) present graphical data for $C_f \cdot Re_{DH}$ as a function of the duct aspect ratio and:

$$C_f \text{ fully developed} = \frac{17.51}{Re_{DH}} \quad (1.1)$$

where the aspect ratio is 0.3 here.

Shah and London (9) discuss the developing nature of the flow in which the friction factor is a function of axial position in the tube. The same authors point out that the more useful quantity is the apparent average friction factor over the development length $C_{f \text{ app}}$. This quantity is a function of aspect ratio where the aspect ratio is defined as:

$$\text{Aspect ratio} = \left(\frac{2a}{2b}\right)$$

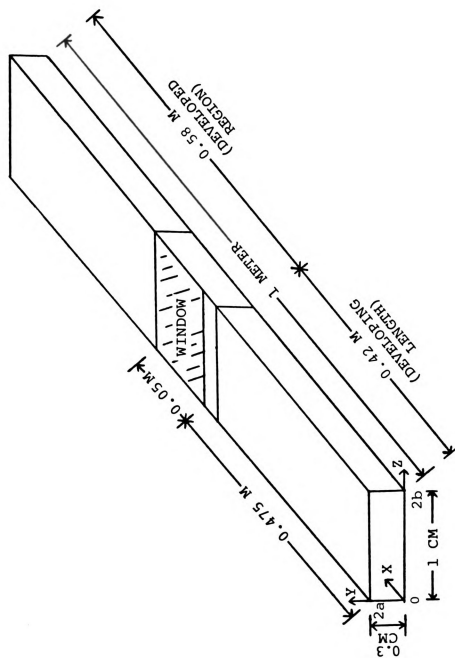


FIGURE 3. DEVELOPING AND DEVELOPED (HYDRODYNAMICALLY) REGIONS

(2a = height of channel; 2b = width of channel)

For the present case, the aspect ratio has a value:

$$\text{Aspect ratio} = 0.3$$

For this value, the apparent friction factor is:

$$C_{f \text{ app}} \cdot \text{Re}_{D_H} = 22.25 \quad (9) \quad (1.2)$$

Therefore:

$$\Delta P_1 = 4 C_{f \text{ app}} \left(\frac{\rho V^2}{2g_c} \right) \frac{X}{D_H} \quad (1.3)$$

$$\Delta P_2 = 4 C_{f \text{ fully developed}} \left(\frac{\rho V^2}{2g_c} \right) \left(\frac{L-X}{D_H} \right) \quad (1.4)$$

where L = length of duct = 1.0 m

Results of the calculation of ΔP for various Reynolds numbers are given in Figure 4. These values are considerably lower than the estimated maximum figures for the flow rate: 1.3×10^{-3} kg/sec, and pressure drop: 9.0×10^3 NT/m², for the turbulent flow in the actual system.

To complete the fluid mechanics description of this model duct flow, we note that the mean velocity of the fluid calculated for $\text{Re}_{D_H} = 1827$ is $\bar{V} = 6.237$ m/sec. The pressure drop per unit length in the fully developed region will be:

$$\frac{dP}{dX} = 4(C_{f \text{ fully developed}}) \frac{\rho V^2}{2g_c} \frac{1}{D_H} = 190.012 \text{ N/m}^3 \quad (1.5)$$

for this case. This information will be used in the solution of the energy equation.

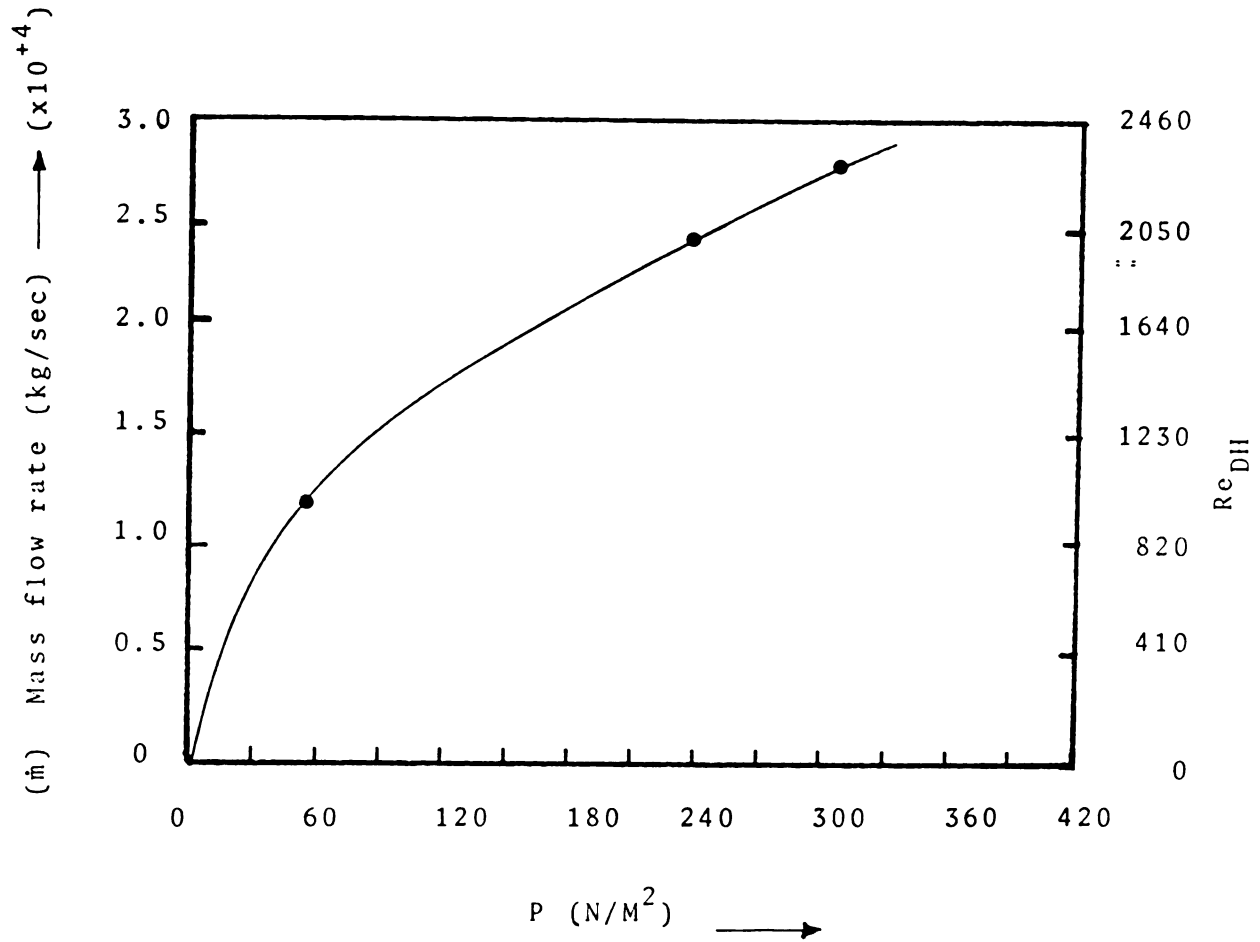


FIGURE 4. REYNOLDS NUMBER AND MASS FLOW RATE AS A FUNCTION OF TOTAL PRESSURE DROP.

Finally, we consider the nature of the thermal boundary layer development in the model system developed here. The non-dimensional thermal length is defined by Shah and London (9) as follows:

$$L_{th}^+ = \frac{L_{th}}{D_H P_e}$$

where L_{th} = duct length from the point of duct heating to the point at which the temperature profile becomes fully developed.

No value of L_{th}^+ was found for the particular case of interest here. However, an estimate of the behavior is obtained by considering laminar flow in a duct with aspect ratio = 0.3 when one wall is maintained at a constant heat flux and the other three walls are maintained at a constant temperature (9). The thermal development length L_{th}^* obtained using this criteria is 41.5 cm, which is much greater than the heater length of interest. Thus the thermal boundary layer will be developing along the heater window surface.

CHAPTER 2

HYDRODYNAMIC CONSIDERATIONS

2.1 NON-DIMENSIONALIZED (FINITE DIFFERENCE) MOMENTUM EQUATION WITH SPECIFIC BOUNDARY CONDITIONS

2.1.1 NON-DIMENSIONALIZED MOMENTUM EQUATION

The velocity field in the fully developed laminar flow (directly beneath the heater surface) is obtained by solving the Navier-Stokes momentum equation in the x-direction (see Figure 3). The solution is developed in non-dimensional form in order to be general and the derivation of the non-dimensional equations from the dimensional form is given in Appendix F.

The non-dimensional momentum equation is given as:

$$\frac{\partial^2 U^+}{\partial y^{+2}} + \frac{\partial^2 U^+}{\partial z^{+2}} = -1$$

where

$$U^+ = \frac{U}{U^*}$$

$$U^* = -\frac{1}{\mu} \left(\frac{dp}{dx} \right) a^2$$

$$y^+ = y/a$$

$$z^+ = z/a$$

and $2a$ is the height of the channel shown in Figure 3.

The boundary conditions applied to this equation are:

- i) $U^+ = 0$ at $y^+ = 0$
- ii) $U^+ = 0$ at $z^+ = 0$
- iii) $\frac{\partial U^+}{\partial z^+} = 0$ at $z^+ = b/a$

2.1.2 FINITE DIFFERENCE APPROACH

A finite difference numerical method of solving

this equation has been applied using the finite difference technique. The finite difference nodal representation of the control volume is given in Figure 5.

In the case where

$$(\Delta y^+)_{\text{n}} = (\Delta z^+)_{\text{e}} = (\Delta y^+)_{\text{s}} = (\Delta y^+)_{\text{w}} = \Delta y^+ = \Delta z^+$$

we get

$$\frac{\partial^2 U^+}{\partial y^{+2}} = \left(\left(\frac{\partial U^+}{\partial y^+} \right)_{\text{n}} - \left(\frac{\partial U^+}{\partial y^+} \right)_{\text{s}} \right) / \Delta y^+ = \left(\frac{U_{\text{n}}^+ - U_{\text{p}}^+}{(\Delta y^+)_{\text{n}}} - \frac{U_{\text{p}}^+ - U_{\text{s}}^+}{(\Delta y^+)_{\text{s}}} \right) / \Delta y^+$$

therefore:

$$\frac{\partial^2 U^+}{\partial y^{+2}} = \frac{U_{\text{n}}^+ - 2U_{\text{p}}^+ + U_{\text{s}}^+}{(\Delta y^+)^2}$$

Similarly:

$$\frac{\partial^2 U^+}{\partial z^{+2}} = \frac{U_{\text{w}}^+ - 2U_{\text{p}}^+ + U_{\text{e}}^+}{(\Delta z^+)^2}$$

Substituting these expressions into the governing equation and simplifying, we get:

$$U_{\text{n}}^+ - 4U_{\text{p}}^+ + U_{\text{s}}^+ + U_{\text{e}}^+ + U_{\text{w}}^+ = -(\Delta y^+)^2 \quad (2.1)$$

2.1.3 METHODS OF SOLUTION

We can solve equation (2.1) by the following methods:

- i) Jacobi Method
- ii) Gauss-Seidel Method
- iii) Gauss-Seidel with S.O.R. Method

These three methods are discussed in Appendix (A). The methods are iterative methods which are used when the problem is two-dimensional and there are large numbers of equations to solve simultaneously. It is very difficult

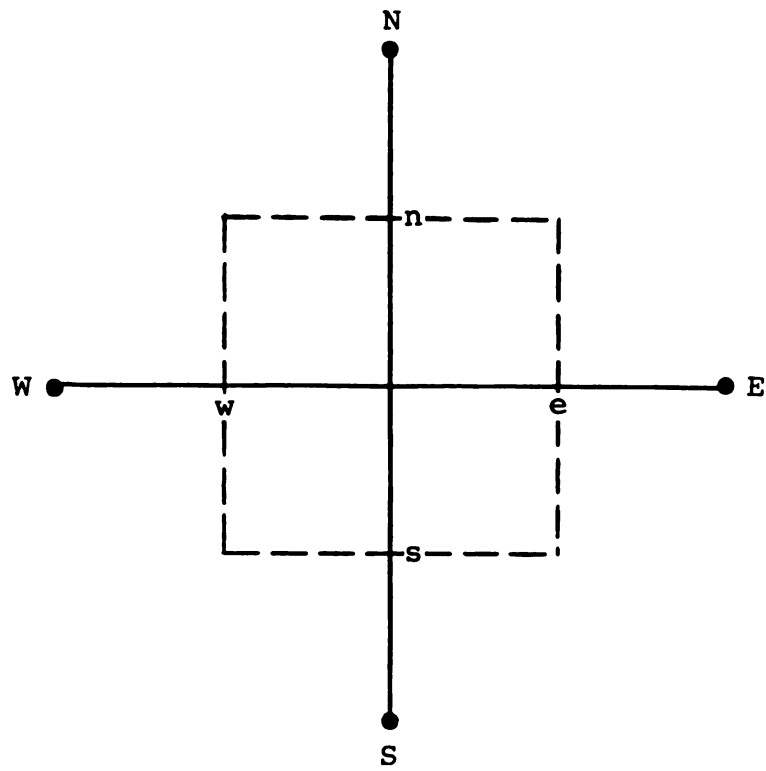


FIGURE 5. FINITE DIFFERENCE CONTROL VOLUME.

to handle two-dimensional equations with large numbers, so iterative methods are used with an initial estimated solution in order to get new values. The rate of convergence of such methods depends on the type of iterative method used. Such iterative methods may not converge at all due to aspects discussed in Appendix (A). Other iterative methods, such as the Alternative Direction Implicit (ADI) Method, can also be used. This method has been used for a solution of the thermal problem (discussed in Appendix (B)). Patankar (3) suggests using the Gauss-Seidel technique with the line-by-line method or the successive overrelaxation method. We will discuss the methods used here and the conditions for convergence will be considered in Appendices (A) and (B).

2.2 HYDRODYNAMIC SOLUTION OF THE PROBLEM

2.2.1 NODAL CONVERSION OF THE FINITE DIFFERENCE EQUATION INTO NODAL FORM

In the previous chapter, we have developed an appropriate non-dimensional finite difference equation for the equation of motion in the 'X' direction:

$$U_n^+ - 4U_p^+ + U_s^+ + U_e^+ + U_w^+ = -(\Delta y^+)^2$$

where U_n^+ , U_s^+ , U_e^+ , U_w^+ , U_p^+ are non-dimensional velocities defined previously and Δy^+ is the non-dimensional distance between nodes.

Due to symmetry about the center line, we only need to take into account one quarter of the rectangular

cross section and determine the velocities at other points within the rectangular cross section. Non-dimensional hydrodynamic boundary conditions are shown in Figure 6 and for our solutions, we define four rows and eleven columns so that

$$\Delta y^+ = \Delta z^+ = 0.333$$

These node arrangements on one quarter of the rectangular cross section in terms of non-dimensional distances are shown in Figure 6.

In this case, equation (2.1) from the previous section will be reduced to

$$U_n^+ - 4U_p^+ + U_s^+ + U_e^+ + U_w^+ = -0.1111 \quad (2.2)$$

Now defining i and j as follows:

i = row number in z^+ direction

j = column number in y^+ direction

we can write this equation in terms of (i,j) as follows:

$$4U^+(i,j) = U^+(i,j+1) + U^+(i,j-1) + U^+(i+1,j) + U^+(i-1,j) + 0.1111$$

with the following boundary conditions

i) $U^+(1,j) = 0, j = 1 \text{ to } 11$

ii) $U^+(i,1) = 0, i = 1 \text{ to } 4$

iii) at $i = 4$:

$$\frac{\partial U^+}{\partial y^+} = 0 \quad \text{so,} \quad \frac{U^+(5,j) - U^+(3,j)}{2(\Delta y^+)} = 0$$

Thus $U^+(5,j) = U^+(3,j), j=1 \text{ to } 11$

iv) at $j = 11$:

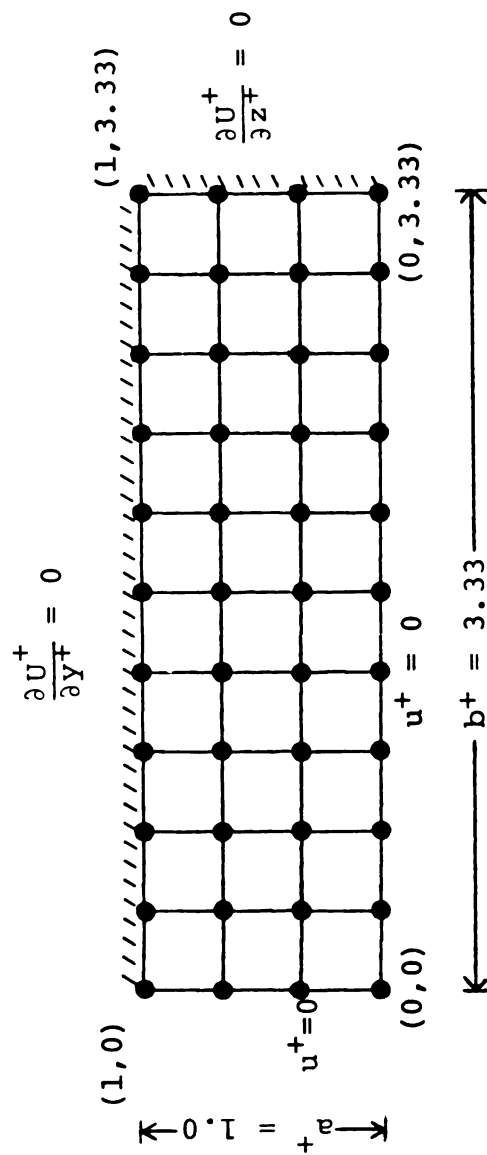


FIGURE 6. NON-DIMENSIONAL HYDRODYNAMIC BOUNDARY CONDITIONS ON RECTANGLE CROSS SECTION QUARTER

$$\frac{\partial U^+}{\partial z^+} = 0, \text{ so } \frac{U^+(i,12) - U^+(i,10)}{2(\Delta z^+)} = 0$$

Thus, $U^+(i,12) = U^+(i,10)$ for $i = 1$ to 4 .

2.2.2 APPROACHES CONSIDERED FOR SOLUTION OF THE MOMENTUM EQUATION

Both the Jacobi and Gauss-Seidel methods of iterative solution were attempted but these techniques failed to yield a convergent solution. However, the successive overrelaxation method was applied in conjunction with the Gauss-Seidel Method and a convergent solution was obtained. The Gauss-Seidel method uses the current value of the unknown obtained in the present iteration stage while the Jacobi method uses the values of the unknown obtained in the previous iteration. The difference between the S.O.R. method and the Gauss-Seidel method is that the S.O.R. method uses an overrelaxation factor (w) for fast convergence of the solution. This factor has a value between one and two while the Gauss-Seidel method could be considered a subset of this method where $w = 1$. The chosen value of the overrelaxation factor between one and two places a variable amount of stress on the importance of the present value of the unknown compared to the previous iteration value. Thus, faster convergence of complex systems of equations is possible as compared to the Gauss-Seidel method. By using the S.O.R. method, a convergent solution was obtained after fifty iterations. The solution is shown in Tables 1 and 2.

The successive overrelaxation factor ' w ' is found

TABLE 1. NON-DIMENSIONAL VELOCITIES $U^+(y^+, z^+)$ AS A FUNCTION OF NON-DIMENSIONAL POSITION

$z^+ \backslash y^+$	0	0.333	0.667	1.00	1.333	1.67	2.0	2.333	2.67	3.0	3.333
0	0	0	0	0	0	0	0	0	0	0	0
0.3	0	0	0	0	0	0	0	0	0	0	0
0.333	0	0.118	0.184	0.222	0.244	0.258	0.266	0.27	0.273	0.274	0.275
0.6	0	0.177	0.284	0.348	0.387	0.41	0.423	0.431	0.436	0.438	0.439
1.0	0	0.195	0.316	0.389	0.433	0.46	0.476	0.485	0.49	0.493	0.4937

TABLE 2. VELOCITIES $U(y, z)$ IN (m/sec)

$z_{cm} \backslash y_{cm}$	0	0.05	0.10	0.15	0.20	0.25	0.30	0.35	0.40	0.45	0.50
0	0	0	0	0	0	0	0	0	0	0	0
0.05	0	2.722	4.245	5.12	5.63	5.95	6.14	6.23	6.30	6.32	6.344
0.10	0	4.08	6.055	8.03	8.93	9.46	9.76	9.95	10.06	10.11	10.13
0.15	0	4.5	7.29	8.97	9.99	10.61	10.98	11.19	11.30	11.31	11.33

using the formulae discussed in Appendix A. The Jacobi, Gauss-Seidel, and S.O.R. methods are discussed in Appendix A along with the respective criteria of convergence.

Using equations (a) and (b) in Appendix A:

$$\delta(B) = \frac{1}{2} (\cos \pi/p + \cos \pi/9)$$

for a unit square mesh of dimension 'h' and a total rectangular cross section of dimensions p_h by q_h , we get in our case,

$$p_h = 1$$

$$q_h = 3.333$$

where $h = \Delta y^+ = \Delta z^+ = 0.333$

$$p = 3 \text{ and } q = 10$$

Substituting the values of p and q above, we get

$$\delta(B) = \frac{1}{2} (\cos \pi/3 + \cos \pi/10) = \frac{1}{2} (0.5 + 0.951) = 0.725$$

Substituting the calculated value of $\delta(B)$ as discussed in the appendix:

$$w_b = \frac{2}{1 + \sqrt{1 - (0.725)^2}} = 1.185$$

The computer program used to solve the hydrodynamic problem, using the successive overrelaxation method along with the Gauss-Seidel method, is given in Appendix D under the name 'HEAT.'

2.2.3 NON-DIMENSIONAL VELOCITIES AT DIFFERENT NON-DIMENSIONAL POSITIONS OBTAINED BY THE PROGRAM 'HEAT'

The results obtained from the computer program after fifty iterations are given in Figure 7.

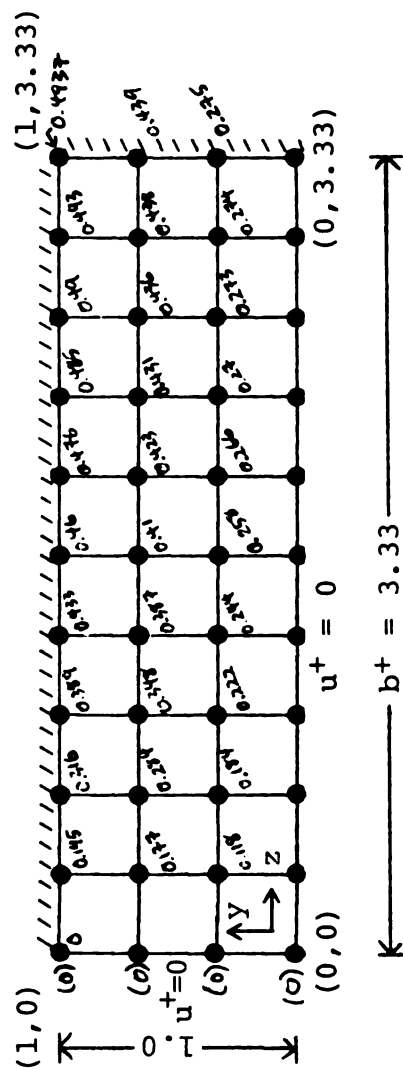


FIGURE 7. NON-DIMENSIONAL VELOCITY AND HYDRODYNAMIC BOUNDARY CONDITIONS ON ONE QUARTER OF THE RECTANGULAR CROSS SECTION

2.2.4 CALCULATION OF VELOCITY AT DIFFERENT POSITIONS IN THE DUCT

To convert the non-dimensional velocities to dimensional velocities at different positions in the y and z directions, we have to first determine the value of (u^*) which is used to non-dimensionalize the x-direction momentum equation. The quantity (u^*) is defined in the previous chapter as follows:

$$u^* = -\frac{1}{\mu} \left(\frac{dp}{dx} \right) a^2 \quad (\text{m/sec})$$

where $a = 0.15$ cm. We have calculated the pressure drop ($\frac{dp}{dx}$) in the previous chapter.

Calculation of the velocity at any position in the fully developed region can now be made from the non-dimensional velocity results obtained from the program:

$$u^* = -\frac{1}{\mu} \left(\frac{dp}{dx} \right) a^2 \quad (\text{m/sec})$$

Substituting the value of $\frac{dp}{dx}$ and a from the previous chapter,

$$-\frac{dp}{dx} = 190.012 \frac{\text{N}}{\text{m}^3} \quad \text{and} \quad a = 0.15 \text{ cm}$$

$$\begin{aligned} u^* &= \frac{1}{\mu \left(\frac{\text{N}}{\text{m}^2} \text{ sec} \right)} \times 190.012 \left(\frac{\text{N}}{\text{m}^3} \right) \times (0.15 \times 10^{-2})^2 (\text{m}^2) \\ &= \left(\frac{1}{18.53 \times 10^{-6}} \times 190.012 \times 0.15 \times 0.15 \times 10^{-4} \right) (\text{m/sec}) \\ &= 23.07 \text{ m/sec} \end{aligned}$$

Thus $u^* = 23.07$ m/sec for the fully developed flow. Calculating the velocities now using the appropriate non-dimensional velocity result and substituting into the following,

$$\frac{u(y,z)}{u^*} = u^+(y,z)$$

where $u^+(y,z)$ is the non-dimensional velocity obtained at a given position.

For example, we are interested in evaluating the velocity at the center of the duct which is the maximum velocity,

$$\frac{u}{u^*} = 0.4937 \text{ (from Figure 7)}$$

$$u_{\text{center}} = 23.07 \times 0.4937 = 11.39 \text{ m/sec}$$

2.2.5 CALCULATION OF FRICTION FACTOR

The friction factor is now calculated from the results in order to compare with the assumption that

$$C_f = \frac{17.51}{Re_{DH}} \text{ for fully developed flow.}$$

We defined the following earlier:

$$u^* = \frac{1}{\mu} \left(\frac{dp}{dx} \right) a^2 \quad (2.3)$$

$$\text{and} \quad \frac{dp}{dx} = 4 C_f \left(\frac{\rho V^2}{2g_c} \right) \frac{1}{D_h} \quad (2.4)$$

Substituting (2.4) into (2.3), we get

$$u^* = 4 C_f \left(\frac{\rho V^2}{2g_c} \right) \left(\frac{a^2}{\mu D_h} \right)$$

so,
$$C_f = \frac{\mu D_h}{2 \rho \left(\frac{V^2}{u^*} \right) a^2}$$

$$C_f = \frac{\mu D_h^2}{2 \rho V^+ V D_h a^2}$$

where $V^+ = u_m/u^*$ and u_m = the mean velocity = V and considering the definition of the Reynolds number,

$$C_f = \frac{D_h^2}{2V^+ (Re) (a^2)}$$

Now to calculate V^+ from the results obtained, the trapezoidal rule is applied which is in final form below.

Since $u_m = \frac{1}{A_c} \int_0^{A_c} u dA_c$ and $U^+ = u/u^*$ where u^* is constant

we derive:

$$V^+ = \frac{1}{A_c} \left[\frac{1}{4} ((U^+) \text{ in corners of the duct}) + \frac{1}{2} (\text{sum of all } U^+ \text{ on the surface of the duct excluding corners}) + (\text{sum of all } U^+ \text{ inside the duct}) \right]$$

In our case, $V^+ = 0.346$ and the computer program calculated friction factor is: $C_f = 14/Re_{DH}$. We believe that the difference between this value and $C_f = 17.51/Re_{DH}$ is due to the finite difference approximations in the solution. The approximation in the integral above is another source of error. No calculations were performed to isolate the difference. This friction factor calculated from the non-dimensional velocity results is less than the Shah and London value by approximately 20%.

2.3 CONCLUSIONS AND COMMENTS ON THE HYDRODYNAMIC SOLUTION

2.3.1 CONCLUSIONS ON APPROACH USED TO SOLVE THE PROBLEM

The hydrodynamic solution for a rectangular duct flow is achieved numerically by the finite difference numerical approach. We observe from the output of the computer program (which is given under the name 'HEAT' in Appendix D) that after forty-eight iterations using the S.O.R. method with the Gauss-Seidel method, convergence is achieved.

The first attempt to solve the problem was using the Jacobi method. A convergent solution was not achieved. This is due to constraints for convergence which are stated in Appendix A. These constraints state that the solution converges only when the coefficient of diagonal element exceeds the sum of the off-diagonal elements.

Another method, which can be used for solution of the finite difference equation, is the Alternative Direction Implicit Method (ADI), which is discussed in Appendix B. Taking large numbers of odd and even steps, in the 'X' direction, after a certain number of steps the solution will be constant for all steps in the 'X' direction, which will reflect the fully developed velocity profile.

Successive overrelaxation is also used for this type of problem and it is a very good alternative to the ADI method, using an optimum overrelaxation factor (w). In the present study, the successive overrelaxation method

is used to solve the hydrodynamic finite difference equation.

2.3.2 CONCLUSIONS AND COMMENTS ON THE SOLUTION ACHIEVED BY THE S.O.R. METHOD

(1) The solution converged after forty-eight iterations.

(2) From Figure 7, we can conclude that at the centerline in the z direction (i.e., $z = 0.5$ cm), the velocity at $y^+ = 1.0$ ($y = 0.15$ cm) is a maximum and the ratio:

$$\frac{U_{\text{center}}}{U_{\text{mean}}} = \left(\frac{23.07}{6.237}\right) \times \left(\frac{\text{computer non-dimensional velocity at center}}{\text{velocity at center}}\right)$$

$$\text{so } \frac{U_{\text{center}}}{U_{\text{mean}}} = \frac{23.07 \times 0.4937}{6.237} = 1.826$$

where $U_{\text{center}} = (u^*) (u^+_{\text{center}})$ and $u^* = 23.07$ m/sec.

Shah and London (9) and Knudson (10) also gave experimental results for rectangular cross sections for the same problem as follows:

$$\frac{U}{U_{\text{max}}} = \left(1 - \left(\frac{y}{6}\right)^n\right) \left(1 - \left(\frac{z}{4}\right)^m\right) \quad (2.5)$$

where $m = 1.7 + 0.5 (\alpha^*)^{-1.4}$

and $n = 2$ for $\alpha^* \leq 1/3$

$= 2 + 0.3(\alpha^* - 1/3)$ for $\alpha^* \geq 1/3$

where $\alpha^* = \text{aspect ratio} = \frac{a}{b} = \frac{0.15}{0.5} = 0.3$

Shah and London (9) also gave the final result of the ratio of maximum velocity to mean velocity as follows:

$$\frac{U_{\max}}{U_m} = \left(\frac{m+1}{m}\right) \left(\frac{n+1}{n}\right) \quad (2.6)$$

$$\text{so, } m = 1.7 + 0.5 (0.3)^{-1.4} = 5.395.$$

Substituting in equation (2.6), we get

$$\frac{U_{\max}}{U_m} = \left(\frac{5.395+1}{5.395}\right) \left(\frac{2+1}{2}\right) = \frac{6.395 \times 3}{5.395 \times 2} = 1.77$$

Comparing the results of the present computer model with the Shah and London value yields a three percent difference:

$$\frac{1.826 - 1.77}{1.77} = 3\%$$

This agreement indicates good agreement between the present computer results and previous work. However, these values may agree without good agreement at the wall (and therefore C_f factors) since U_{\max} and U_m are less sensitive to the approximations made at the boundary than the actual boundary values themselves would be.

(3) If we consider Figures 8 and 9, the wall gradient of velocity in the z^+ direction is smaller than the gradient of velocity in the y^+ direction. This is

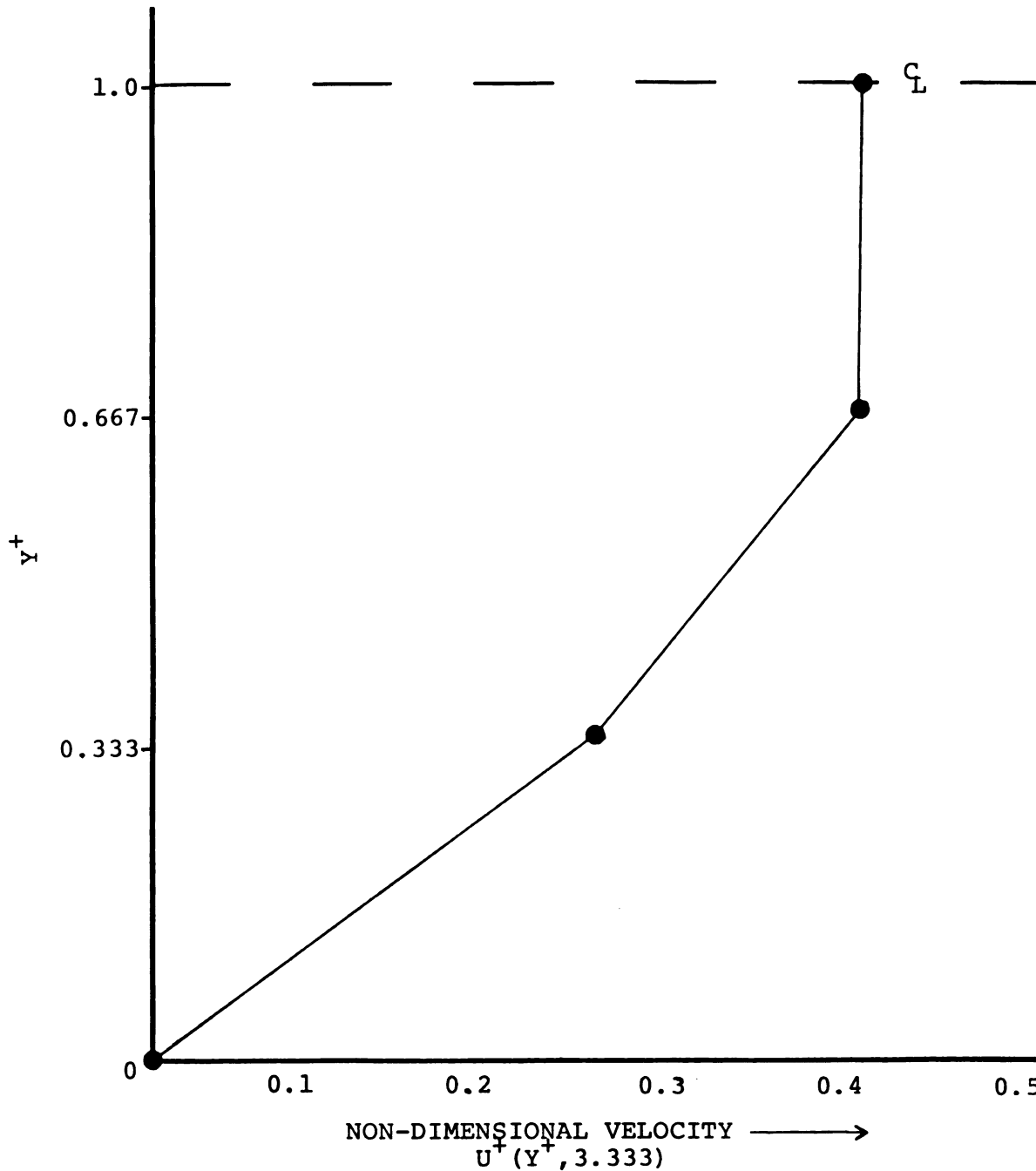
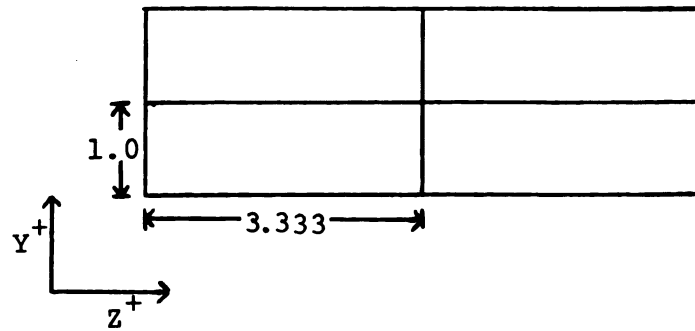


FIGURE 8. FINITE DIFFERENCE APPROXIMATION OF THE NON-DIMENSIONAL VELOCITY VARIATION IN y^+ DIR^N AT $z^+ = 3.333$

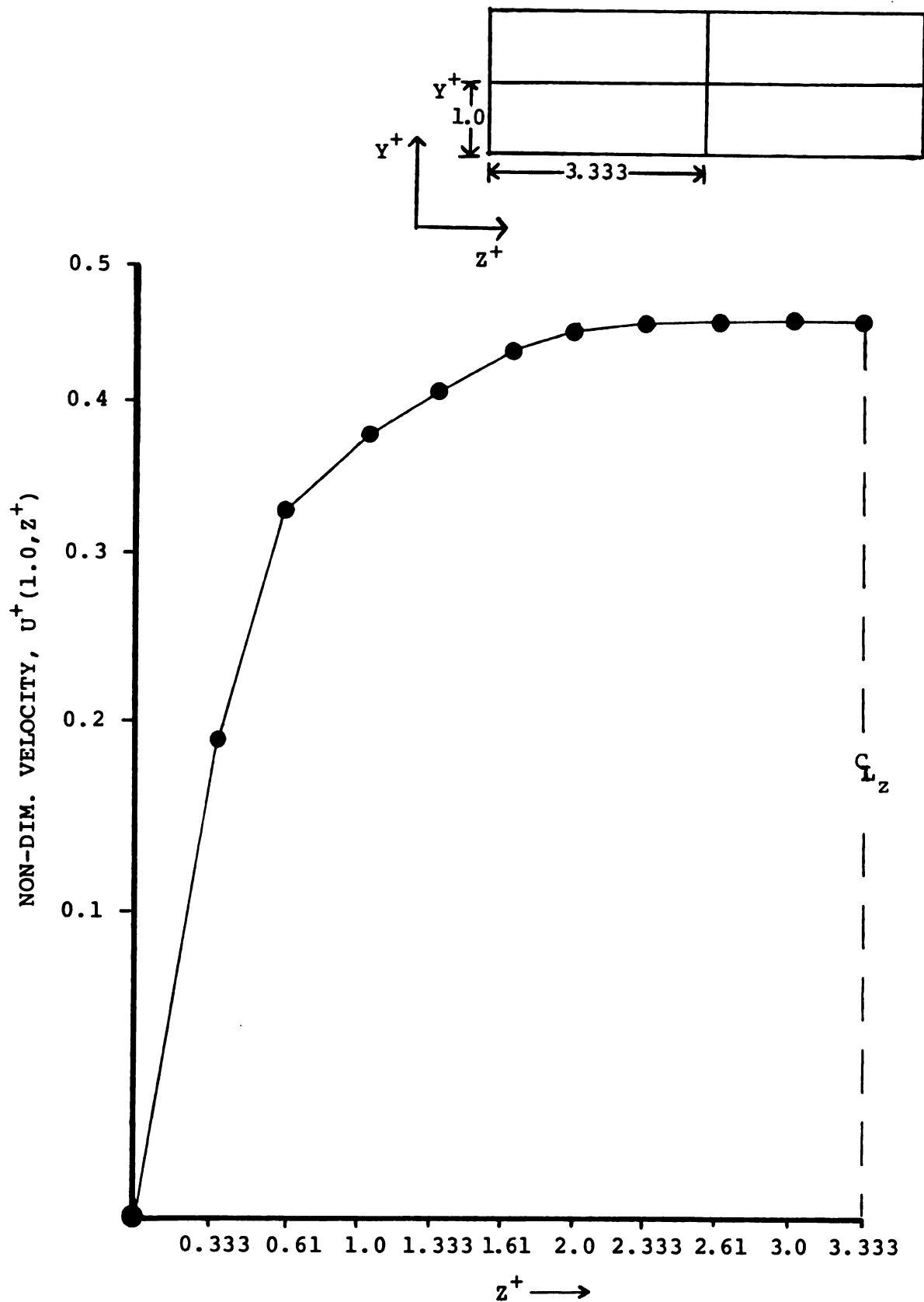


FIGURE 9. FINITE DIFFERENCE APPROXIMATION OF THE VARIATION OF NON-DIMENSIONAL VELOCITY IN z^+ DIRECTION AT $y^+ = 1.0$

due to the fact that the viscous stress in the z^+ direction is less than the viscous stress in the y^+ direction (i.e.,

$$\frac{\partial u}{\partial y} > \frac{\partial u}{\partial z} \text{) .}$$

CHAPTER 3
THERMAL CONSIDERATIONS

3.1 DIMENSIONAL APPROACH FOR THE THERMAL SOLUTION OF THE PROBLEM

Although a non-dimensional solution to the energy equation could be developed as was the case for the velocity field, only a dimensional solution is presented at this time for the specific model system presented here.

3.1.1 INTRODUCTION

As described in Chapter 2, the present problem is assumed to consist of boundary conditions on each side of the cross section as follows:

(1) three sides of the rectangular cross section are insulated, i.e. $q'' = 0$

(2) on one side of the rectangular cross section, $q'' = \text{constant}$ (axially and laterally)

The boundary conditions are shown in Figure 10. The sole thermocouple used in the cryomicroscope system is placed on the center of the window heater typically and this is shown in Figure 10, where the position is denoted by " β ."

The energy equation for hydrodynamically fully developed flow and thermally developing flow is derived by the control volume approach and is discussed by Kays and Crawford (8):

$$U \frac{\partial T}{\partial X} = \alpha \left(\frac{\partial^2 T}{\partial X^2} + \frac{\partial^2 T}{\partial Y^2} + \frac{\partial^2 T}{\partial Z^2} \right) \quad (3.1)$$

where $\alpha \frac{\partial^2 T}{\partial X^2}$ is the axial conduction term.

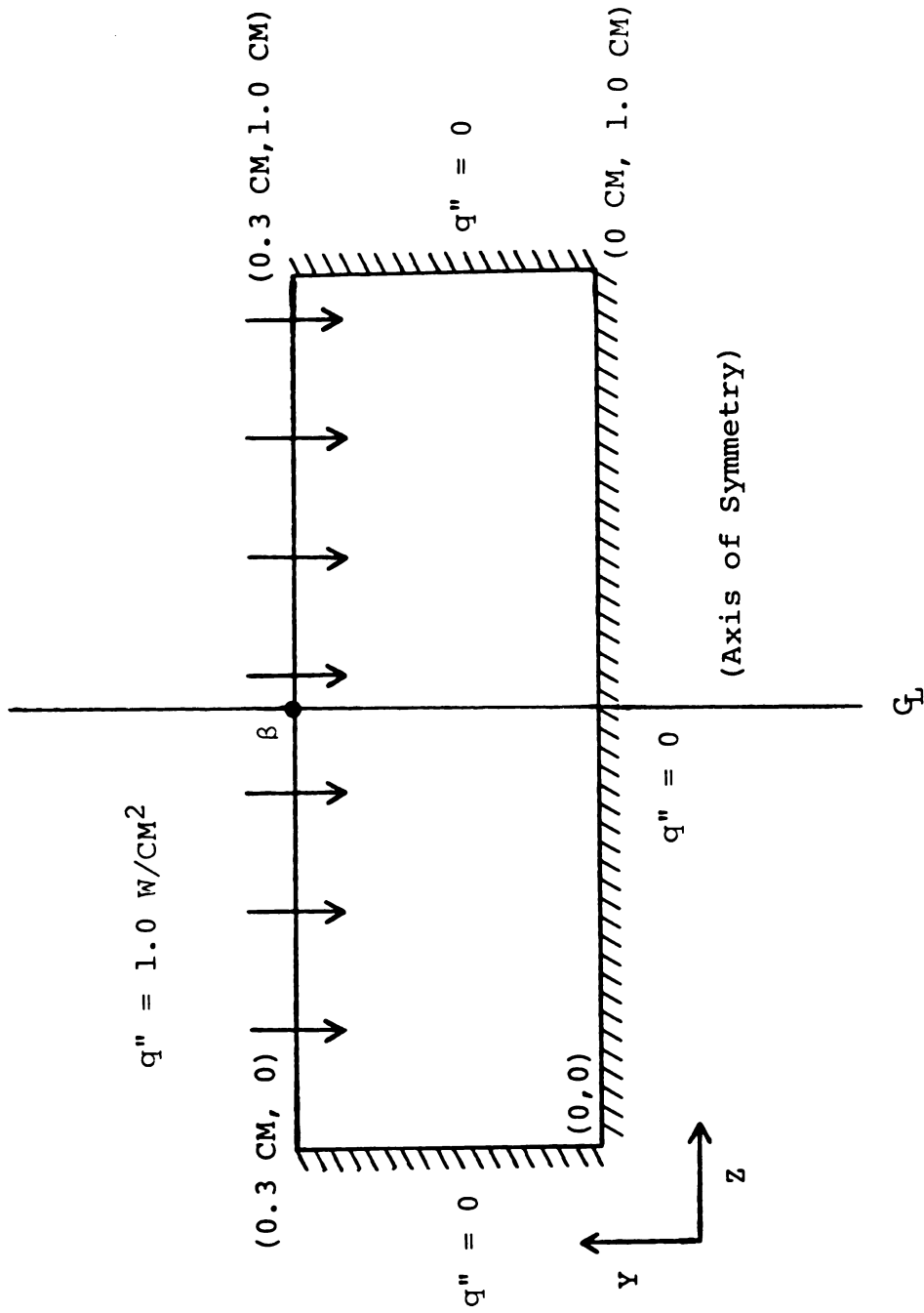


FIGURE 10. THERMAL BOUNDARY CONDITIONS ON SURFACES OF RECTANGLE DUCT

Analyzing the energy equation by an order-of-magnitude analysis, and defining the magnitudes of order:

$$x \propto (L)$$

$$y \propto (a)$$

$$z \propto (a)$$

$$u \propto (U_m)$$

$$\text{so,} \quad U \frac{\partial T}{\partial X} \propto \left(\frac{U_m T}{L} \right)$$

$$\frac{\partial^2 T}{\partial x^2} \propto \left(\frac{T}{L^2} \right)$$

$$\frac{\partial^2 T}{\partial y^2} \propto \left(\frac{T}{a^2} \right)$$

$$\frac{\partial^2 T}{\partial z^2} \propto \left(\frac{T}{a^2} \right)$$

Now, comparing the magnitude of the axial conduction terms with the lateral conduction terms since $a = 0.15$ cm and $L = 5$ cm (i.e., 0.05 m), the lateral conduction terms are dominating terms compared to the axial conduction term. So the axial conduction term is neglected. The axial conduction term is only important within the short length from the leading edge of the heater where the temperature gradients are significant. This is a standard procedure. Robert Hornbeck (12) neglected the axial conduction term when the flow is developing both hydrodynamically and thermally. Vera Preingingerova (12, 13) also neglected the axial conduction term for rectangular ducts with various aspect ratios. V. Gastri (15) also supports the argument of neglecting the axial conduction term while solving

numerically the problem for the square duct with various boundary conditions. Therefore:

$$U \frac{\partial T}{\partial x} = \alpha \left(\frac{\partial^2 T}{\partial y^2} + \frac{\partial^2 T}{\partial z^2} \right) \quad (3.2)$$

This is a three-dimensional problem where

$U \neq f(x)$ because the velocity profile is fully developed, but

$U = f(y, z)$, and

$T = f(x, y, z)$ as the temperature profile is developing

Boundary Conditions:

- (i) at $x = 0$, i.e., at the leading edge of the window, the temperature of the fluid in the duct is 23°C
- (ii) $q''|_{z=0} = -k \frac{\partial T}{\partial z} = 0 = q''|_{z=b}$
- (iii) for $y = 0$, $q''|_{y=0} = -k \frac{\partial T}{\partial y} = 0$
- (iv) at $y = 0.3 \text{ cm}$, $q''|_{y=0.3 \text{ cm}} = -k \frac{\partial T}{\partial y}|_{y=0.3 \text{ cm}}$

$$= \frac{5 \text{ W}}{5 \times 1 \text{ cm}^2} = 1 \frac{\text{W}}{\text{cm}^2}$$

3.1.2 FINITE DIFFERENCE APPROACH

Converting equation (3.1) into the finite difference form similar to the conversion of the momentum equation:

$$\frac{T_N - 2T_P + T_S}{(\Delta y)^2} + \frac{T_E + T_W - 2T_P}{(\Delta z)^2} = \frac{U_P}{\alpha} (T_{P_{x+\Delta k}} - T_{P_x}^*)$$

where T_p^* is the value of the temperature at the previous iteration. This equation is solved by the Alternative Direction Implicit (ADI) method which is described in Appendix B.

The finite difference network for this system is shown in Figure 11.

Boundary Conditions:

(i) at $x = 0$, i.e., first step in the ADI method,

$$T(I, J, 1) = 23.0$$

(ii) for given step $J = 1$ (i.e., on boundary $z = 0$)

$$q'' \Big|_{z=0} = -k \frac{\partial T}{\partial z} \Big|_{z=0} = 0, \text{ so } T(I, 2, J1) = T(I, 0, J1)$$

$$\text{and similarly at } z = b \quad k \frac{\partial T}{\partial z} \Big|_{z=b} = 0 = q'' \Big|_{z=b}$$

Considering the finite difference cross section as in Figure 11 where $\Delta z = \Delta y = 0.05$ cm and $\Delta x = 0.2$ cm

(iii) for $y = 0$, $q'' \Big|_{y=0} = -k \frac{\partial T}{\partial y} \Big|_{y=0} = 0$, so

$$T(2, J, J') = T(0, J, J') \text{ in our approach}$$

(iv) For $y = 0.3$ cm, $q'' \Big|_{y=0.3 \text{ cm}} = -k \frac{\partial T}{\partial y} \Big|_{y=0.3 \text{ cm}}$

$$= 1 \text{ w/cm}^2, \text{ so } T(8, J, J1) - T(6, J, J1)$$

$$= 2(\Delta y)^{\text{cm}} \times \frac{q}{k} \frac{\text{w/cm}^2}{\frac{\text{w}}{\text{mx}^{\circ}\text{C}} \times \frac{\text{m}}{\text{cm}}} = 382.55^{\circ}\text{K}$$

According to the ADI method described in Appendix B, for even steps,

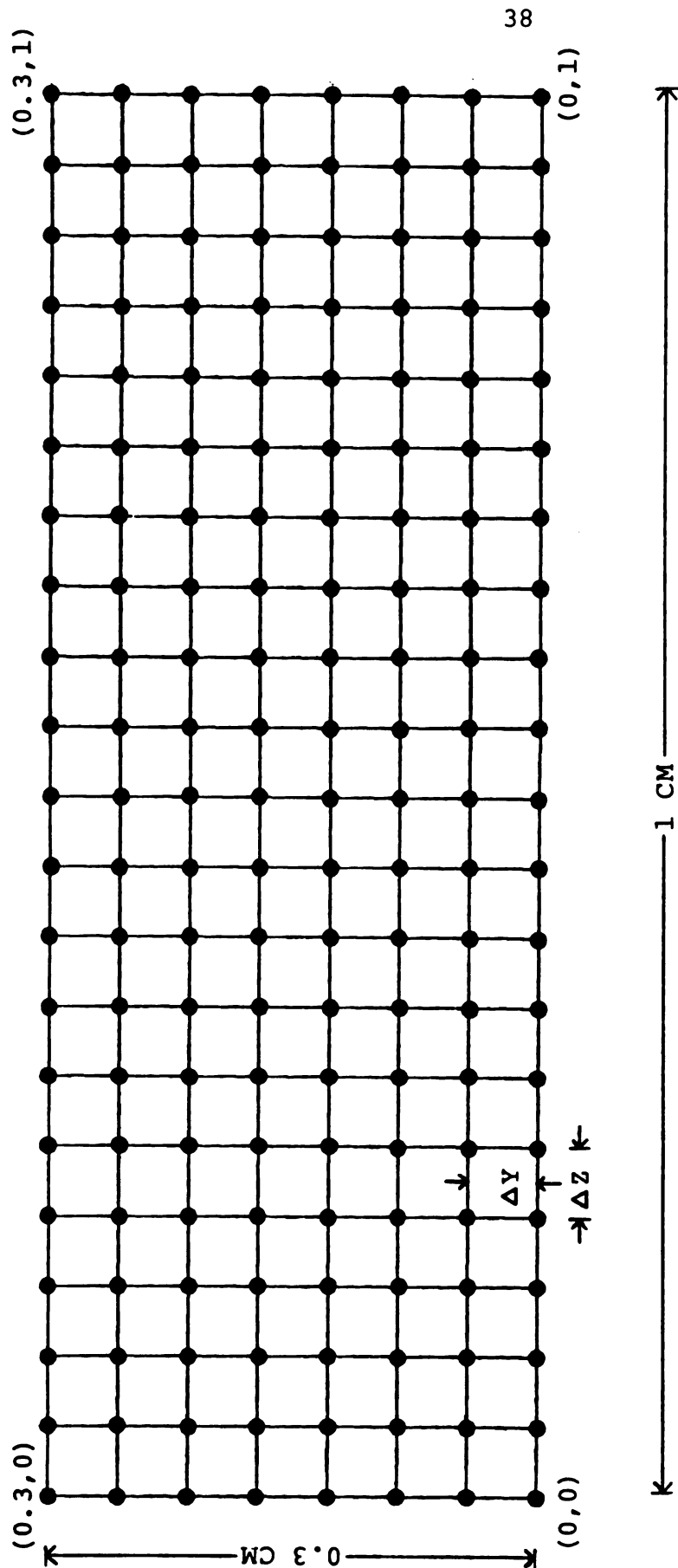


FIGURE 11. FINITE DIFFERENCE CROSS SECTION FOR THERMAL SOLUTION.

$$\left. \frac{\partial^2 T}{\partial z^2} \right|_{x+\Delta x} + \left. \frac{\partial^2 T}{\partial y^2} \right|_x = \frac{u}{\alpha} \left(\frac{T_{x+\Delta x} - T_c}{\Delta x} \right)$$

and in finite difference form,

$$\frac{T_N - 2T_P + T_E}{(\Delta z)^2} + \frac{T_N^O - 2T_P^O + T_S^O}{(\Delta y)^2} = \frac{U(I,J)}{\alpha} \left(\frac{T_P - T_P^O}{\Delta x} \right)$$

In our program

$$\left(\frac{U(I,J)}{\alpha} \right) \left(\frac{y^2}{\Delta x} \right) = R(I,J) = \text{constant at given position}$$

So our finite difference equation for even steps will be

$$T_N + T_E + T_N^O + T_S^O + (R(I,J) - 2) T_P^O = (R(I,J) + 2) T_P \quad (3.3)$$

For odd steps,

$$\left. \frac{\partial^2 T}{\partial z^2} \right|_x + \left. \frac{\partial^2 T}{\partial y^2} \right|_{x+\Delta x} = \frac{U}{\alpha} \left(\frac{T_{x+\Delta x} - T_x}{\Delta x} \right)$$

and similarly as described in even steps, the finite difference form of the energy equation will be as follows:

$$T_W^O + T_E^O + T_N + T_S + (R(I,J) - 2) T_P^O = (R(I,J) + 2) T_P \quad (3.4)$$

The thermal entry length problem was solved by digital computer using the finite difference equations by the ADI method. The only difficulty which was encountered was that on the sides of the rectangular cross section, the velocity is actually zero but the finite difference

equations must account for the convection properly near the wall. Therefore, due to the linearity considered in the finite difference equation while formulating the problem, the velocity at the wall at a given point is assumed to be:

$$U_{(se)} = \frac{U_P + U_E + U_S + U_S'}{4} \quad (\text{see Figure 12})$$

A similar procedure is used for $U_{(ne)}$, $U_{(nw)}$, and $U_{(sw)}$. After calculating all the velocities above, U_P is calculated:

$$U_P = \frac{U_{(se)} + U_{(sw)} + U_{(nw)} + U_{(ne)}}{4}$$

This linear approach is assumed because throughout the study, $(\Delta y = \Delta z)$ is considered.

3.2 THERMAL PROBLEM SOLUTION BY THE FINITE DIFFERENCE APPROACH

3.2.1 INTRODUCTION

We have discussed the assumptions and the dimensional approach to the thermal problem of interest in the previous section. We have applied the Alternative Direction Implicit (ADI) method for this three-dimensional problem which is discussed in Appendix B, along with the TDMA method which is discussed in Appendix C. The governing equation is formulated in finite difference form along with the boundary conditions in the previous chapter. The computer program which is designed to solve this problem is given in Appendix E under the name "Convection Program."

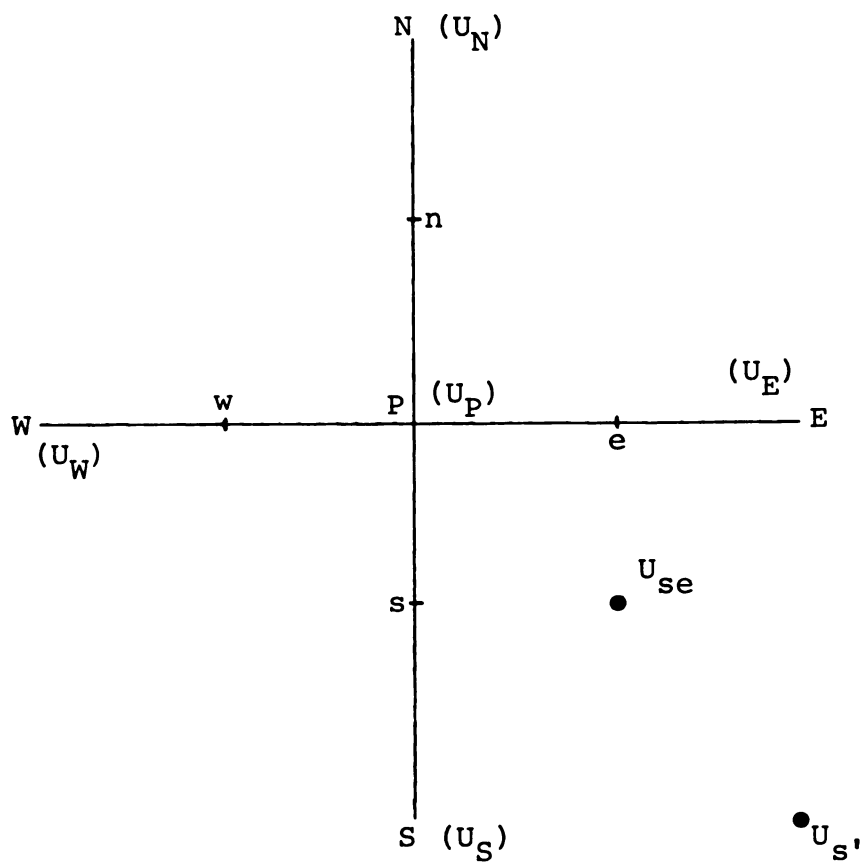


FIGURE 12. VELOCITY ASSUMPTION IN CALCULATING VELOCITY ON BOUNDARY FOR THERMAL SOLUTION.

In solving the problem by the convection program, the $R(I,J)$ values which are defined in the previous chapter as $R(I,J) = \left(\frac{U(I,J)}{\alpha} \frac{(\Delta y)^2}{\Delta x} \right)$ are calculated and shown in Figure 13 and used in the program. The computer results are shown in Table 3 at different y and z positions as a function of the x direction. The thermocouple is placed along the centerline of the window. The predicted variation of temperature at the centerline location of the thermocouple is shown in Table 4 with respect to the x direction (i.e., distance from the leading edge).

3.2.3 CALCULATION OF MEAN FLUID TEMPERATURE AT EXIT OF WINDOW REGION

The mean temperature of the fluid at $x = 5$ cm is calculated in order to perform an energy balance on the system for examining the validity of the calculated solution. The trapezoidal rule in two dimensions is used as given below. We can use the Simpson rule also by modifying it for two dimensions according to Hornbeck (12). It is quite accurate to use the Simpson rule for hydrodynamically and thermally developing flow in the rectangular duct (12). The mean temperature is defined in the general case by Kays and Crawford (8) which is as follows:

$$T_M = \frac{1}{A_c U_m} \int_{A_c} UT dA_c$$

$$T_M = \frac{1}{A_c U_m} \int_0^b \int_0^a UT \cdot dy \cdot dz$$

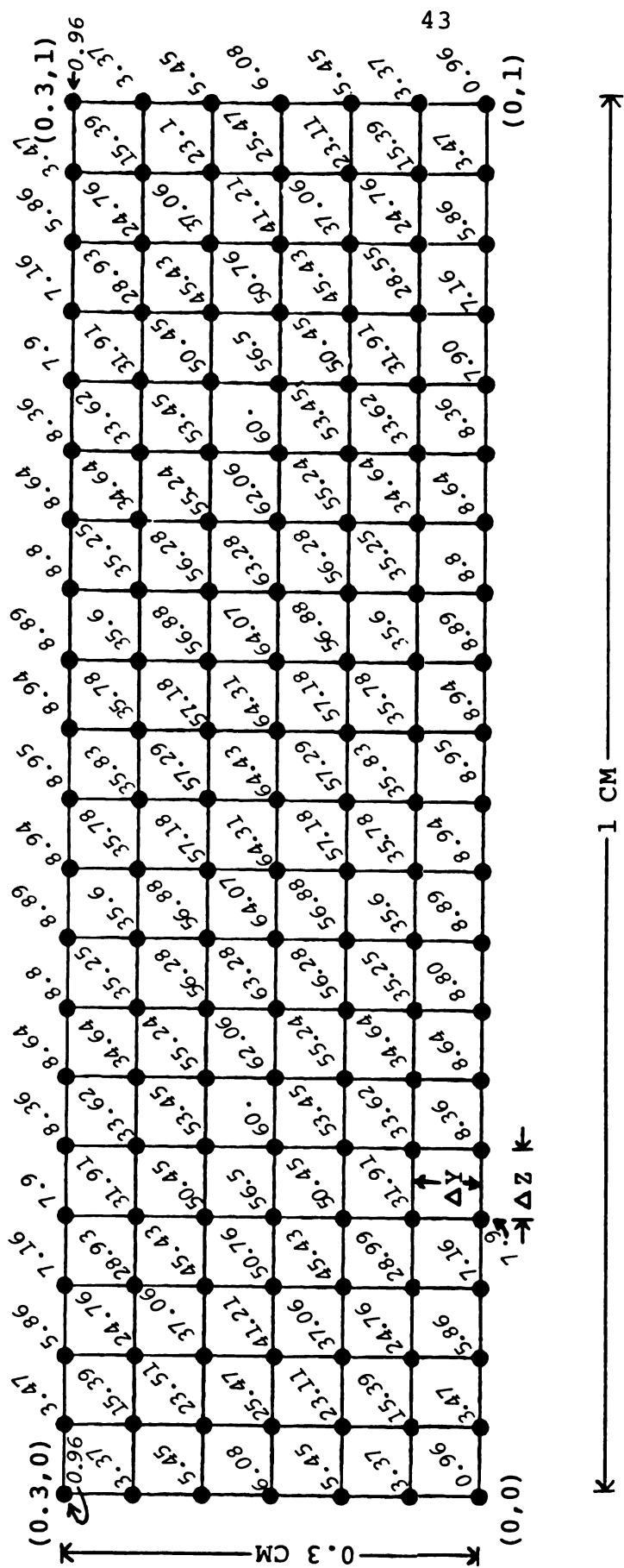


FIGURE 13. NON-DIMENSIONAL TEMPERATURE PARAMETER $R(I,J)$ USED IN THE A D I METHOD FOR SOLVING THE ENERGY EQUATION

3.2.2 RESULTS OBTAINED BY COMPUTER PROGRAM 'CONVECTION.'

TABLE 3. TEMPERATURES AT DIFFERENT LOCATIONS IN THE RECTANGULAR DUCT AT VARIOUS DISTANCES FROM THE LEADING EDGE OF THE HEATER.

$x = 0 \text{ cm}$							
$\frac{z}{Y \text{ cm}}$	$Y \text{ cm}$	0	0.1	0.2	0.3	0.4	0.5
0		23.00	23.00	23.00	23.00	23.00	23.00
0.05		23.00	23.00	23.00	23.00	23.00	23.00
0.1		23.00	23.00	23.00	23.00	23.00	23.00
0.15		23.00	23.00	23.00	23.00	23.00	23.00
0.20		23.00	23.00	23.00	23.00	23.00	23.00
0.25		23.00	23.00	23.00	23.00	23.00	23.00
0.30		23.00	23.00	23.00	23.00	23.00	23.00

TABLE 3, continued

x = 1 cm

$\begin{matrix} z \text{ cm} \\ y \text{ cm} \end{matrix}$	0	0.1	0.2	0.3	0.4	0.5
0	23.1	23.0	23.0	23.0	23.0	23.0
0.05	23.16	23.00	23.0	23.00	23.00	23.0
0.10	23.64	23.00	23.0	23.00	23.00	23.0
0.15	26.28	23.05	23.01	23.00	23.00	23.0
0.2	39.64	24.11	23.46	23.36	23.39	23.33
0.25	95.63	42.62	34.88	33.30	32.84	32.73
0.30	252.22	195.68	165.74	157.62	155.14	154.57

TABLE 3, continued

x = 2 cm

$\begin{array}{c} z \\ y \end{array}$ cm	0	0.1	0.2	0.3	0.4	0.5
0	23.3	23.02	23.00	23.00	23.00	23.0
0.05	23.55	23.02	23.00	23.00	23.00	23.0
0.10	24.97	23.05	23.01	23.00	23.00	23.0
0.15	31.26	23.48	23.12	23.08	23.08	23.076
0.20	56.25	28.64	25.38	24.90	24.77	24.74
0.25	135.73	73.30	55.59	51.69	50.54	50.28
0.30	301.28	248.34	220.35	212.10	209.57	208.98

TABLE 3, continued

 $x = 3 \text{ cm}$

$\frac{z \text{ cm}}{y \text{ cm}}$	0	0.1	0.2	0.3	0.4	0.5
0	23.88	23.10	23.0	23.00	23.00	23.00
0.05	24.33	23.07	23.01	23.00	23.00	23.00
0.10	27.06	23.24	23.03	23.02	23.02	23.02
0.15	37.53	24.69	23.45	23.32	23.29	23.29
0.20	72.36	36.25	28.98	27.82	27.51	27.44
0.25	164.34	101.54	76.6	70.74	69.02	68.63
0.30	331.96	281.10	250.25	241.49	238.88	238.28

TABLE 3, continued

x = 4 cm

$\frac{z}{y}$ cm	0	0.1	0.2	0.3	0.4	0.5
0	24.50	23.28	23.02	23.00	23.00	23.00
0.05	25.31	23.23	23.02	23.00	23.00	23.00
0.10	29.48	23.67	23.09	23.06	23.05	23.05
0.15	44.04	26.77	24.07	23.78	23.71	23.69
0.20	87.21	45.61	33.82	31.80	31.25	31.13
0.25	188.50	126.48	94.25	88.67	86.48	85.98
0.30	358.26	307.83	273.58	263.54	260.64	259.98

TABLE 3, continued

x = 5 cm

$\frac{z}{y}$ cm	y cm					
	0	0.1	0.2	0.3	0.4	0.5
0	25.667	23.58	23.05	23.01	23.01	23.01
0.05	26.75	23.52	23.04	23.02	23.01	23.01
0.10	32.52	24.41	23.23	23.14	23.13	23.126
0.15	51.08	29.70	25.07	24.51	24.38	24.35
0.20	101.13	55.94	39.66	36.52	35.82	35.63
0.25	208.73	148.46	114.28	105.16	102.55	101.96
0.30	379.57	330.83	293.67	282.17	278.86	278.117

TABLE 4. TEMPERATURE OF THE HEATER CENTERLINE AS A
FUNCTION OF DISTANCE FROM THE LEADING EDGE
OF THE HEATER.

x cm	Temp. of Thermocouple ($^{\circ}\text{C}$)
0	23.00
0.2	58.10
0.6	116.12
1.0	154.57
1.4	181.19
1.8	200.63
2.2	215.63
2.6	227.85
3.0	238.28
3.4	247.52
3.8	255.94
4.2	263.76
4.6	271.12
5.0	278.12

According to the trapezoidal rule for one direction (ref. 18) for:

$$\left(\int_0^a U \cdot T dy \right) = \frac{\Delta y}{2} (f_0 + 2f_1 + 2f_2 + \dots + 2f_{n-1} + f_n)$$

where $f = f(i, j)$ and in our case $f_0, f_1, f_2, \dots, f_n$ are values of (UT) at $y = 0, \Delta y, 2\Delta y, 3\Delta y, \dots, n\Delta y$. Now integrating again with respect to the z direction:

$$T_m = \frac{1}{A_C U_m} \frac{y}{2} \cdot \frac{z}{2} \left[f(0, 0) + 2f(0, \Delta z) \dots + 2f(0, (m-1)\Delta z) + f(0, m\Delta z) \right. \\ \left. + 2(f(\Delta y, 0) + 2(\Delta y, \Delta z) \dots + 2f(\Delta y, (m-1)\Delta z) + f(\Delta y, m\Delta z)) \right. \\ \left. + 2(f(n-1)\Delta y, 0) + 2f(n-1)\Delta y, \Delta z) \dots + f(n-1)\Delta y, m\Delta z) \right) \\ \left. + f(n\Delta y, 0) + 2f(n\Delta y, \Delta z) \dots + f(m\Delta y, m\Delta z) \right]$$

The product (UT) at different locations is given in Figure 14.

Because of the symmetry about the center line in the z direction of our problem, using the trapezoidal rule, where

$$U_m = V = 6.237 \text{ m/sec}$$

$$A_C = 0.3 \times 1 \times 10^{-4} \text{ m}^2$$

$$\Delta y = \Delta z = 0.05 \text{ m}$$

we can calculate ' T_m ' from the half cross section as follows:

$$T_m = \frac{2\Delta y \cdot \Delta z}{A_C U_m} \left[\frac{1}{4} (UT(7, 0) + UT(1, 0)) + \frac{1}{2} (\text{sum of product} \right.$$

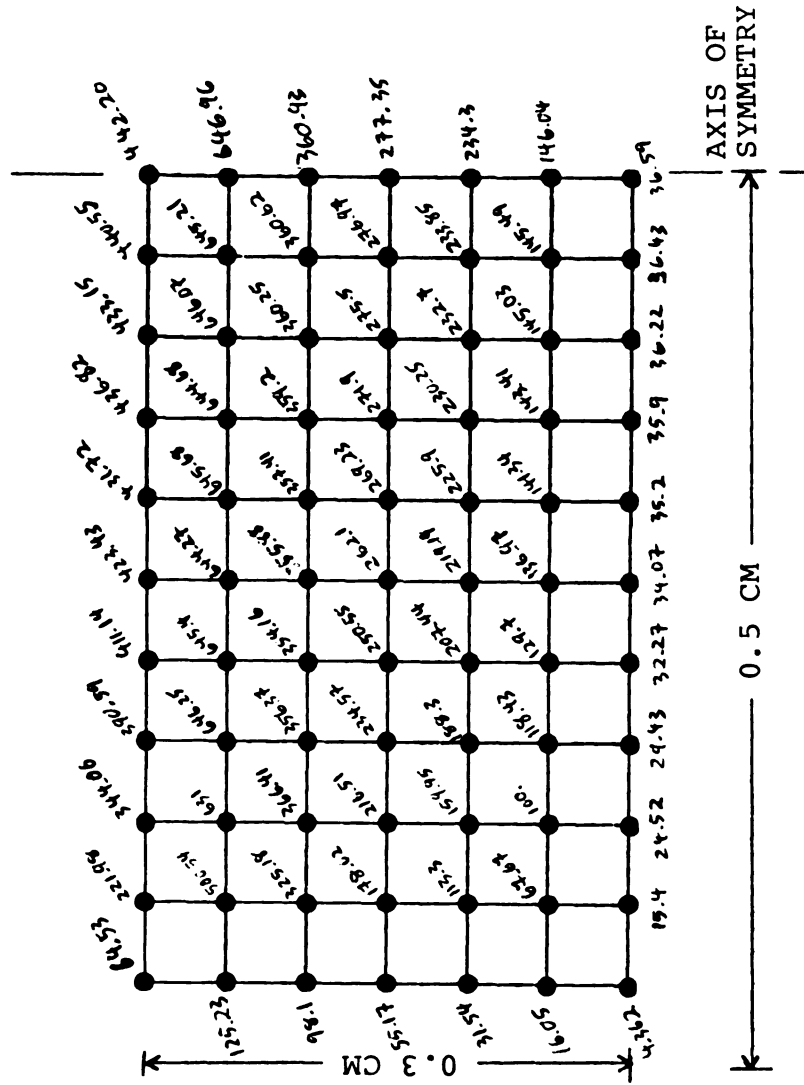


FIGURE 14. THE PRODUCT OF VELOCITY AND TEMPERATURE (UT) AT DIFFERENT NODES IN THE DUCT AT THE TRAILING EDGE OF THE WINDOW ($x = 5$ CM)

(UT) at all nodes on boundary $y=0$, $z=0$, $y=0.3$ cm) + (sum of product (UT) at all nodes inside the cross section)]

Calculating the mean temperature from Figure 14 using the above approach, we get:

$$T_m = 48.1^{\circ}\text{C}$$

This value will be compared to that computed from a first law energy balance. The lateral variation (in the z direction) of temperature on the window at given distances from the leading edge of the heater is shown in Figure 15.

In Figure 16, the variation of the centerline temperature at different distances from the leading edge of the heater is shown.

3.3 CONCLUSIONS AND COMMENTS ON THE THERMAL SOLUTION

3.3.1 GENERAL COMMENTS ON THE RESULTS

The solution to the energy equation with the specified thermal boundary conditions is discussed and presented in the previous chapter. This solution was obtained by using the finite difference method with the ADI approach. Figure 15 shows the variation of temperature at different lateral positions on the window surface at given distances from the leading edge. Figure 16 shows the centerline temperature variation (of the thermocouple) from the leading edge of the window. The following conclusions are derived from the results obtained from the computer program:

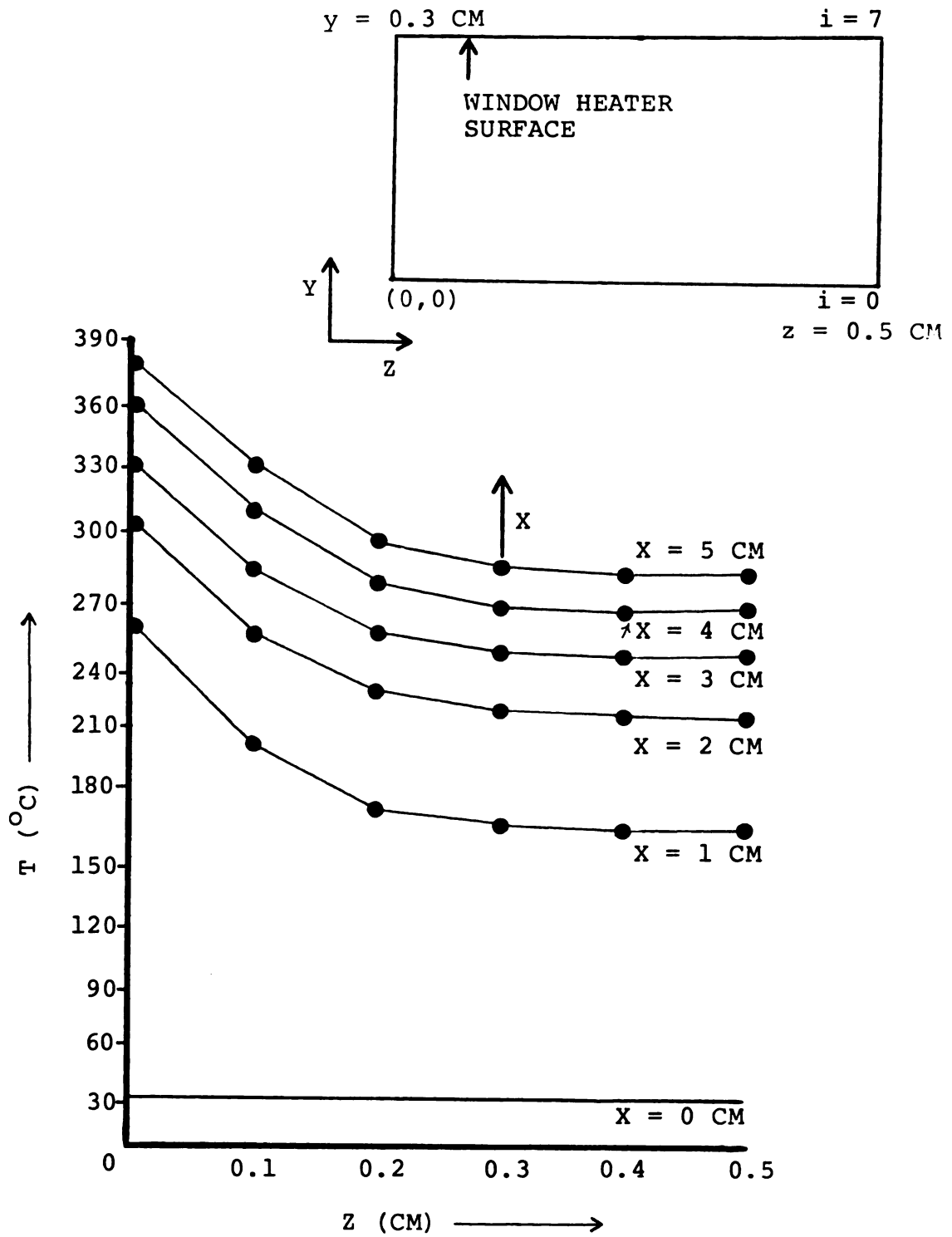


FIGURE 15. PREDICTED VARIATION OF TEMPERATURE AT WINDOW HEATER SURFACE IN 'Z' DIRECTION AT A GIVEN 'X'

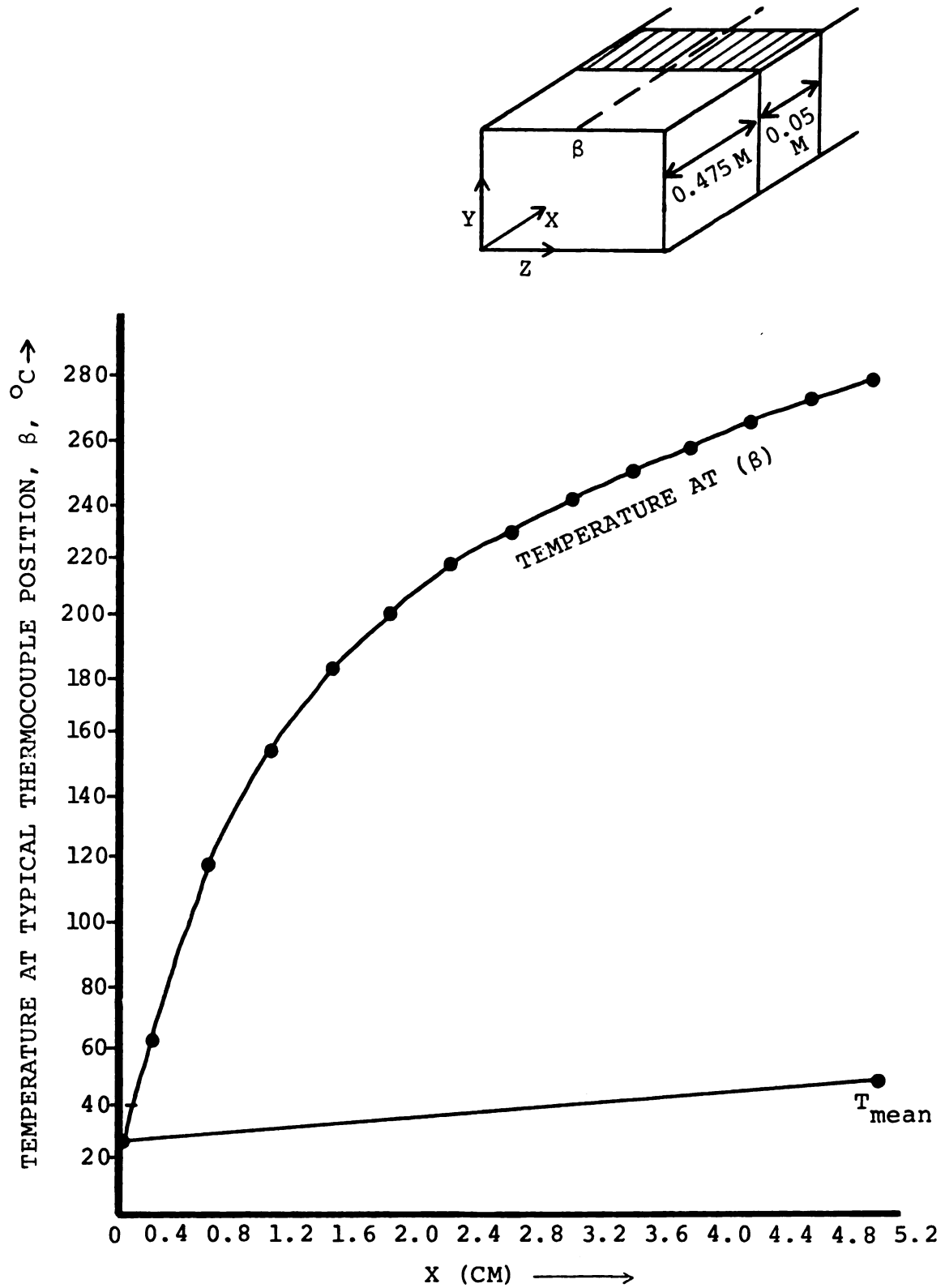


FIGURE 16. VARIATION OF THERMOCOUPLE TEMPERATURE WITH DISTANCE FROM LEADING EDGE

1) On the window surface, the temperature varies both laterally and axially. The lateral variation is shown in Figure 15. The lateral temperature gradient ($\frac{\partial T}{\partial z}$) depends on the position in the rectangular cross-section. To illustrate the magnitude of these gradients we calculate the approximate gradient at $x = 1$ cm:

$$\begin{aligned}\left. \frac{\partial T}{\partial z} \right|_{x=1 \text{ cm}} &= \frac{T(0.3, 0.1) - T(0.3, 0.0)}{\Delta z} \\ &= \frac{195.68 - 252.22}{0.1} = \frac{-56.54}{0.1} = -565.4^{\circ}\text{C/cm}\end{aligned}$$

Examining the results of Table 3 indicates that the largest lateral thermal gradients appear closest to the beginning of the heated length. This region warrants a closer examination in future work.

The maximum temperature gradients in the x direction are also a function of distance from the leading edge of the heater because of the developing temperature profile. The maximum axial temperature gradient also occurs at the leading edge of the heater and is approximately:

$$\begin{aligned}\left. \frac{\partial T}{\partial x} \right|_{\text{max}} &= \frac{T(0.4, 0.3, 0.5) - T(0.0, 0.3, 0.5)}{0.4} \\ &= \frac{58.10 - 23.00}{0.2} = 175.5^{\circ}\text{C/cm}\end{aligned}$$

The temperature gradients in the x direction (i.e., axial direction) decrease with distance from the leading edge of the heater.

2) The temperature at the leading edge is 23°C

while temperature at the trailing edge of the window is different for different locations on the window surface. However, the maximum temperature is always at the corners of the duct near the heater window.

3) The temperature at the centerline increases rapidly within one centimeter from the leading edge, then the gradient decreases considerably. As shown in Figure 16 the mean temperature of the fluid increases linearly, a consequence of the first law for uniform heat flux. The fact that the slopes of $\frac{\partial T_{\text{mean}}}{\partial x}$ and $\partial T_{\beta} / \partial x$ do not match over the length of the heater (5 cm) indicates that the flow is still thermally developing at $x = 5$ cm which confirms our earlier estimate predicting that this would be the case.

4) The temperature along the line ' β ' where the thermocouple is typically placed is the minimum temperature on the surface of the window at a given distance from the leading edge of the window.

5) We have neglected the axial conduction term while solving numerically the thermal problem, which is justified on an order of magnitude basis. The Peclet number in our case is equal to $1827 \times 0.72 (=Re \cdot P_r) = 1315$ which is much higher than five (5). The axial conduction term can be neglected for cases having Peclet numbers more than '5' as discussed in Kays and Crawford (9).

3.3.2 ENERGY BALANCE CHECK OF THE RESULTS

Checking our solution with the help of the energy balance by the first law of thermodynamics which

states that for the steady state

energy in = energy stored + energy out

$$\text{i.e., } \dot{m} C_p \Delta T = Q \quad (3.5)$$

where $\Delta T = T_{b2} - T_{b1}$

T_{b2} = mean bulk fluid temperature at trailing edge of window surface

T_{b1} = mean bulk fluid temperature at the leading edge of the window. $(\text{kg/m}^3) (\text{m}^2)$

$$\begin{aligned} \text{In our case, } \dot{m} &= \rho \times A \times V \text{ (m/sec) (kg/sec)} \\ &= 1.1766 \text{ (kg/m}^3\text{)} \times 0.3 \times 10^{-4} \text{ (m}^2\text{)} \\ &\quad \times 6.237 \text{ (m/sec)} \\ &= 2.207 \times 10^{-4} \text{ (kg/sec)} \end{aligned}$$

$$c_p = 1.005 \times 10^3 \text{ joule/kg}^\circ\text{K}$$

$$Q = 5 \text{ watts}$$

Substituting into equation (3.5), we get

$$\Delta T = \frac{Q}{\dot{m} C_p} = \frac{5 \text{ (w)}}{2.207 \times 10^{-4} \text{ (kg/sec)} \times 1.005 \times 10^3 \left(\frac{\text{w} \cdot \text{sec}}{\text{kg}^\circ\text{K}} \right)}$$

$$\Delta T = T_{b2} - T_{b1} = 22.70^\circ\text{C}$$

$$T_{b2} = 22.70 + 23.0 = 45.70^\circ\text{C}$$

In the previous chapter, the solution technique for mean temperature was discussed. We can use either the trapezoidal rule or Simpson rule in two dimensions to calculate the mean temperature at the trailing edge (i.e., $x = 5$ cm). Using an approximate method, i.e., trapezoidal method, the mean bulk temperature at the trailing edge

is calculated in the previous chapter and it is equal to 48.1°C , i.e., $T_{b2} = 48.1^{\circ}\text{C}$.

Comparing the mean bulk temperature obtained by the energy balance and by the finite difference method, they are quite close and the error of the finite difference solution is:

$$\frac{48.1 - 45.70}{45.70} = \frac{T_{b2}(\text{finite diff.}) - T_{b2}(\text{energy bal.})}{T_{b2}(\text{energy balance})}$$

$$= 5.3\%$$

This error is due in part to the velocity approximation on the surfaces of the duct and the approximate solution technique (i.e., alternative direction implicit) to solve the thermal problem with specified boundary conditions. The trapezoidal method of solving the mean temperature at the trailing edge of the window is also approximate. Though the error in the velocity solution is multiplied by the error in the temperature solution, i.e.,

$$\text{error in (UT)} = (\text{error in } u)(\text{error in } T)$$

the error as a whole is 5.3% which is acceptable for our present purposes.

6) This problem for a variety of boundary conditions is also solved by V. Preingerova and P. H. G. allen (14) by a dimensionless approach for both thermally and hydrodynamically developing flow. However, the problem was solved for

quite a small magnitude of length in developing and developed (hydrodynamically) region.

3.3.3 COMMENT ON PARALLEL PLATE APPROXIMATIONS

Comparing the actual rectangular duct solution with a parallel plate approximation solution which is discussed below, we can examine the conclusion given by Hornbeck (12) which states that if the aspect ratio is less than '5', a parallel plate approximation is rejected in order to avoid misleading results for a rectangular duct flow. There are two methods of solving the parallel plate problem which are considered here and discussed by Kays and Crawford (9), who give an hydraulic diameter approach tabular form to solve the flow behavior through the parallel plate. Cess and Shaffer (16) used the analytical approach in which the parallel plates are heated equally axially but at different levels of heat flux on each plate. For our approach U_m should be calculated for Reynolds number = 1827 according to the parallel plate approximation,

$$Re = 1827 = \frac{4 \times a \text{ (m)} \times U_m \text{ (m/sec)}}{v \text{ (m}^2\text{/sec)}}$$

where $D_n = 4a$ (for parallel plate)

$$U_m = 4.8 \text{ m/sec}$$

Now defining the Peclet number:

$$Pe = \frac{4U_m a}{\alpha} \frac{\text{(m/sec)m}}{\text{m}^2\text{/sec}}$$

where $\alpha = 22.106 \times 10^{-6} \text{ m}^2/\text{sec}$ (in our case)

Then $Pe = 1315$

Now using the graph which is derived analytically for

$(\frac{1}{Pe} \frac{x}{a})$, as a function of $\frac{T_{wi} - T_b}{(\frac{q_1 a}{k})}$ for $q_2 = 0$ (i.e.,

one side heated and one side insulated), we get the following results:

TABLE 5. RESULTS BY CESS AND SHAFFER METHOD.

x cm	$T_{wi} - T_b (^{\circ}t)$	$T_b (^{\circ}C)$	$T_{wi} (^{\circ}C)$
0	0	23.0	23.0
0.5	116.68	28.37	144.85
1.0	146.32	33.74	180.06
2.0	188.2	44.78	232.68
3.0	220.36	55.25	275.60
4.0	245.6	65.95	311.55
5.0	263.98	74.54	338.50

Kays and Crawford also obtain results for the same problem using the hydraulic diameter approach and obtain very similar results. Comparing our solution for the flow in the rectangular duct which is given for point ' β ' in Table 4 and the parallel plate solution by Cess and Shaffer which is given in Table 5, we conclude that the results are quite different for a given aspect ratio if we were to simplify the problem using a parallel plate assumption

and the solution will be misleading in all respects.
So for an aspect ratio less than five, the effect of
corners are significant and cannot be neglected.

CHAPTER 4

DISCUSSION AND CONCLUSIONS

4.1 DISCUSSION AND CONCLUSIONS

A preliminary quantitative understanding of the temperature gradients on the heater surface of a convective cryomicroscope heat transfer system has been realized by developing a simplified model of the actual complex situation.

The primary aim of the present study was to consider the effects of the developing thermal boundary layer with respect to the thermal gradients on the window heater surface. The numerical solution to this simplified problem, to the best of our knowledge, represents the first solution to a thermally developing, laminar boundary layer in a rectangular duct of aspect ratio 0.3 with constant heat flux on one wall and with the other three walls insulated. The solution is in qualitative agreement with experimental results obtained by Hrycaj on the actual complex system indicating very large thermal gradients in the axial direction. (See Figure 2.) Furthermore, the present model predicts severe thermal gradient problems in the lateral direction as well as the axial direction. (See Figures 15 and 16.)

The velocity field solution has been checked by calculating the friction factor, C_f , in the hydrodynamically fully developed region and the ratio $(U_{\max}/U_{\text{mean}})$ and comparing these values with those available in Shah and London(9). We find that there is excellent agreement with the values of $(U_{\max}/U_{\text{mean}})$ (<1% difference), but that the present computed values of $C_f \cdot \text{Re}_{\text{DH}}$ differ by approximately

20% as compared to the published values of $C_f \cdot Re_{DH}$ for this case. We feel that this difference is due to the finite difference approximations made near the wall of the duct. These approximations are likely to affect the wall velocity gradients, wall shear, and thus C_f to a larger degree than the effects on the ratio of (U_{max}/U_{mean}) . No attempt was made to vary the number of nodes near the wall or to make variations of the finite difference approximations to test this assertion. This should be done in future research extending this work.

The energy equation was checked by calculating an enthalpy-mean temperature (or bulk temperature) difference across the heated section of the duct. The difference in enthalpy convected across the heated section matches the heat transfer into the duct to within 1%. This indicates satisfaction of the first law. However, judging by the results obtained in the solution of the velocity field we might expect that the mean temperature effects may be well matched without necessarily obtaining acceptable accuracy locally. Thus the heater surface temperature which is affected by the local velocity gradients may be in error by a magnitude comparable to that estimated for the friction factor (20%). This should be checked in future work.

4.2 SUGGESTIONS FOR FUTURE WORK

There are several relevant modifications of the current computer program that are needed in order to make the model more representative of the actual convection type

of cryomicroscope stage used by Hrycaj. The computer program can also be used for thermal design purposes, given any particular model.

In the latter category there are several relatively minor program changes that would allow parameter studies of the effect of a non-uniform heat flux from the heater window. It would also be straightforward to change the present rectangular heater configuration to a circular geometry to match the actual system. Finally, the adiabatic boundary conditions on the two sides and the bottom of the duct could be relaxed to include natural convection boundary conditions as more realistic conditions for the actual stage. Along these same lines we should change the heater boundary condition from one of uniform heat flux into the refrigerant fluid to heat generation in the thin film with convection into the refrigerant fluid as well as conduction and/or convection from the heater into the sample placed on top of it. Variable fluid properties are easily incorporated into the present computer model to check for the effects of this factor.

In the former category we can mention three factors which should be taken into account in order to make the computer model more accurately match the actual system. These factors will be more difficult to achieve than those already mentioned.

Firstly it will be necessary to incorporate the effects of simultaneously developing flow in order to

make it possible to consider thermal designs which place the heater in a hydrodynamically developing region.

Secondly we should include those flow geometries which may induce separation, and lastly we would like to understand quantitatively what the effects of turbulent flow will be on the temperature field on the top heater surface.

In the actual operation of the convection heat transfer stage the transient characteristics of the system play an important role and these effects should be considered in future work.

APPENDICES

APPENDIX A. METHODS OF ITERATION

(A.1) Jacobi Method of Iteration (ref. 4)

If we denote first approximation to x_i by $x_i^{(1)}$ and second by $x_i^{(2)}$, etc., I assume that 'n' iterations are to be carried out. Then Jacobi iterative method expresses the $(n+1)^{th}$ iterative values exclusively in terms of n^{th} iterative values and they are as follows:

If the equations are

$$a_{11}x_1 + a_{12}x_2 + a_{13}x_3 + \dots + a_{1m}x_m = b_1 \quad (A.1)$$

$$a_{21}x_1 + a_{22}x_2 + a_{23}x_3 + \dots + a_{2m}x_m = b_2 \quad (A.2)$$

$$a_{31}x_1 + a_{32}x_2 + a_{33}x_3 + \dots + a_{3m}x_m = b_3 \quad (A.3)$$

etc. and there are 'n' equations like A.1, A.2 and A.3.

In general, applying the Jacobi method,

$$x_1^{(n+1)} = \frac{1}{a_{11}} (b_1 - a_{12}x_2^{(n)} - a_{13}x_3^{(n)} \dots - a_{1m}x_m^{(n)})$$

$$x_2^{(n+1)} = \frac{1}{a_{22}} (b_2 - a_{21}x_1^{(n)} - a_{23}x_3^{(n)} \dots - a_{2m}x_m^{(n)})$$

$$x_3^{(n+1)} = \frac{1}{a_{33}} (b_3 - a_{31}x_1^{(n)} - a_{32}x_2^{(n)} \dots - a_{3m}x_m^{(n)})$$

So in general case for 'm' equations,

$$x_i^{(n+1)} = \frac{1}{a_{ii}} (b_i - \sum_{j=1}^{i-1} a_{ij}x_j^{(n)} - \sum_{j=i+1}^m a_{ij}x_j^{(n)}), \quad i = 1(1)m$$

The condition for the convergence of Jacobi iterative method if the i^{th} equation of $AX = B$ is,

$$a_{i1}x_1 + a_{i2}x_2 + \dots + a_{ii}x_i + \dots + a_{im}x_m = b_i$$

Then Jacobi iteration will converge if,

$$|a_{i1}| + |a_{i2}| + \dots + |a_{i,i-1}| + 0 + |a_{i,i+1}| + \dots + |a_{im}| < |a_{ii}|$$

This states that the Jacobi method applies to equation $AX = B$ will converge if 'A' is diagonally dominant matrix, i.e., if in each row of 'A', the modulus of the diagonal element exceeds the sum of the moduli of the off-diagonal elements.

(A.2) GAUSS-SEIDEL METHOD

Jacobi method uses the previous iteration value to calculate the present iterative value. Unlike Jacobi method, Gauss Seidel method uses the (n+1)m iterative values as soon as they are available and the iteration corresponding to the equation

$$a_{11}x_1 + a_{12}x_2 + a_{13}x_3 + a_{14}x_4 \dots + a_{1m}x_m = b_1$$

$$a_{21}x_1 + a_{22}x_2 + a_{23}x_3 + a_{24}x_4 \dots + a_{2m}x_m = b_2$$

and so on up to

$$a_{m1}x_1 + a_{m2}x_2 + a_{m3}x_3 + a_{m4}x_4 + \dots + a_{mm}x_m = b_m$$

are defined by

$$x_1^{(n+1)} = \frac{1}{a_{11}} (b_1 - a_{12}x_2^{(n)} - a_{13}x_3^{(n)} - a_{14}x_4^{(n)} \dots - a_{1m}x_m^{(n)})$$

$$x_2^{(n+1)} = \frac{1}{a_{22}} (b_2 - a_{21}x_1^{(n+1)} - a_{23}x_3^{(n)} - a_{24}x_4^{(n)} \dots - a_{2m}x_m^{(n)})$$

$$x_3^{(n+1)} = \frac{1}{a_{33}} (b_3 - a_{31}x_1^{(n+1)} - a_{32}x_2^{(n+1)} - a_{34}x_4^{(n)} \dots - a_{3m}x_m^{(n)})$$

and so on up to

$$x_m^{(n+1)} = \frac{1}{a_{mm}} (b_m - a_{m1}x_1^{(n+1)} - a_{m2}x_2^{(n+1)} - a_{m3}x_3^{(n+1)} \dots - a_{m(m-1)}x_{(m-1)}^{(n+1)})$$

In general case for m equations,

$$x_i^{(n+1)} = \frac{1}{a_{ii}} (b_i - \sum_{j=1}^{i-1} a_{ij}x_j^{(n+1)} - \sum_{j=i+1}^m a_{ij}x_j^{(n)}), \quad i=1(1)m.$$

THE CONDITION FOR CONVERGENCE OF GAUSS-SEIDEL ITERATIVE MODEL:

The condition for convergence of Gauss-Seidel method is given by the Scarborough Criterion which indicates that a sufficient condition for the convergence of the Gauss Seidel method is

$$\frac{\sum |a_{im}|}{|a_{ii}|} < \text{for all equations}$$

$$< \text{for at least one equation } (m \neq i)$$

This condition is described by Patanker (ref. 3, pp. 64).

This is the similar condition which is used for convergence of Jacobi iterative method.

A.3 GAUSS SEIDEL WITH S.O.R. METHOD (SUCCESSIVE OVERRELAXATION)

This method of iteration is suggested for use in comparison to the previous page, we have discussed Gauss Seidel equations which can be written as follows also:

$$x_1^{(n+1)} = x_1^{(n)} + \left(\frac{1}{a_{11}} (b_1 - a_{11}x_1^{(n)} - a_{12}x_2^{(n)} - a_{13}x_3^{(n)} - a_{14}x_4^{(n)} - \dots - a_{1m}x_m^{(n)}) \right)$$

$$x_2^{(n+1)} = x_2^{(n)} + \left(\frac{1}{a_{22}} (b_2 - a_{21}x_1^{(n+1)} - a_{22}x_2^{(n)} - a_{23}x_3^{(n)} - \dots - a_{2m}x_m^{(n)}) \right)$$

and so on up to

$$x_m^{(n+1)} = x_m^{(n)} + \left(\frac{1}{a_{mm}} (b_m - a_{m1}x_1^{(n+1)} - a_{m2}x_2^{(n+1)} - \dots - a_{m(m-1)}x_{m-1}^{(n+1)} - a_{mm}x_m^{(n)}) \right)$$

If successive corrections are all one signed as they usually are for the approximating difference equations of elliptic problems. It would be reasonable to expect convergence to be accelerated if each above equation was given larger correction term than is defined by above equations. This is called successive overrelaxation or S.O.R. iteration which is defined by equations as follows:

$$x_1^{(n+1)} = x_1^{(n)} + \frac{w}{a_{11}} (b_1 - a_{11}x_1^{(n)} - a_{12}x_2^{(n)} - a_{13}x_3^{(n)} \dots \\ - a_{1m}x_m^{(n)})$$

and so on up to

$$x_m^{(n+1)} = x_m^{(n)} + \frac{w}{a_{mm}} (b_m - a_{11}x_1^{(n+1)} - a_{12}x_2^{(n+1)} \dots \\ - a_{1m}x_m^{(n)})$$

In general, for m equations, S.O.R. Iteration is defined as follows:

$$x_i^{(n+1)} = x_i^{(n)} + \frac{w}{a_{ii}} (b_i - \sum_{j=1}^{i-1} a_{ij}x_j^{(n+1)} - \sum_{j=i}^m a_{ij}x_j^{(n)}), \quad i=1(1)m$$

The above equation can be simplified and written as follows:

$$x_i^{(n+1)} = \frac{w}{a_{ii}} (b_i - \sum_{j=1}^{i-1} a_{ij}x_j^{(n+1)} - \sum_{j=i+1}^m a_{ij}x_j^{(n)}) - (w-1)x_i^{(n)}$$

The factor w' in above equations is called acceleration parameter or relaxation factor. It generally lies in the range $1 < w < 2$. The determination of the optimum value of 'w' for maximum rate of convergence will be discussed in the next topic. The value $w=1$ gives Gauss Seidel Iteration.

This method is also suggested by Robert Hornbeck (ref. 5) at National Aeronautical Research Center for developing flow hydrodynamically in rectangle duct which is quite complicated problem compared to fully developed flow (hydronamically) in solving large number of two-dimensional equations simultaneously.

Patankar (ref. 3) suggests on page 66 that to solve the two-dimensional conduction problem of similar formulation as above formulations, S.O.R. method with line-by-line method which is described in the same book by the author.

TO CALCULATE THE OPTIMUM RELAXATION FACTOR 'w'

Smith (ref. 4) gives the following criteria to decide optimum overrelaxation factor for S.O.R. method (page 252):

$$\rho(B) = \frac{1}{2} \left(\cos \frac{\pi}{p} + \cos \frac{\pi}{q} \right) \quad (A)$$

for square mesh of side 'h' and for rectangular cross section of sides 'ph' and 'qh' using five point difference approximation and

$$w_b = \text{optimum relaxation factor} = \frac{2}{1 + \sqrt{(1 - \rho^2(B))}} \quad (B)$$

where $\rho(B)$ is the spectral radius of the Jacobi method iteration matrix.

This condition is discussed by Smith in detail on pp. 243-50.

Roache in his book Computational Fluid Dynamics also suggested above approach by Smith for calculating successive overrelaxation factor (w) which is given on pp. 118 in the same book.

APPENDIX B: ADI METHOD

The equation we used in thermal solution of the problem in general is three-dimensional equation and it is as follows:

$$\frac{\partial^2 \phi}{\partial z^2} + \frac{\partial^2 \phi}{\partial y^2} = R(I, J) \frac{d\phi}{dx}$$

For the 1st, 3rd, ... (odd) steps in x direction,

$$\left. \frac{\partial^2 \phi}{\partial z^2} \right|_x + \left. \frac{\partial^2 \phi}{\partial y^2} \right|_{x+\Delta x} = R(I, J) \frac{\phi_{x+\Delta x} - \phi_x}{\Delta x}$$

where $R(I, J)$ is constant and it is either dependent on position or not according to the problem to be solved. In finite difference form, taking Figure 5 into account,

$$\frac{\phi_w^o - 2\phi_p^o + \phi_e^o}{(\delta z)^2} + \frac{\phi_n - 2\phi_p + \phi_s}{(\delta y)^2} = R(I, J) \frac{\phi_p - \phi_p^o}{S_x}$$

In our case if $\Delta z = \Delta y$, then the above equation is resulted in the following final form for odd steps in x direction:

$$\phi_w^o - 2\phi_p^o + \phi_e^o + \phi_n - 2\phi_p + \phi_s = \frac{R(I, J) (\Delta y)^2}{\Delta x} (\phi_p - \phi_p^o) \quad (A)$$

For the 2nd, 4th (even) steps in x direction:

$$\left. \frac{\partial^2 \phi}{\partial z^2} \right|_{x+\Delta x} + \left. \frac{\partial^2 \phi}{\partial y^2} \right|_x = R(I, J) \left(\frac{\phi_{x+\Delta x} - \phi_x}{\Delta x} \right)$$

and simplifying into finite difference form,

$$\frac{\phi_w - 2\phi_p + \phi_e}{(\delta z)^2} + \frac{\phi_n^o - 2\phi_p^o + \phi_s^o}{(\delta y)^2} = \frac{R(I,J)}{\delta x} (\phi_p - \phi_p^o)$$

and if $S_z = S_y$, we get the final finite difference equation for even space steps in x direction as follows:

$$\phi_w - 2\phi_p + \phi_e + \phi_n^o - 2\phi_p^o + \phi_s^o = \frac{R(I,J)(\Delta y)^2}{\Delta x} (\phi_p - \phi_p^o) \quad (B)$$

In above equations (A) and (B), we used o superscript which denotes the present time and no superscript means future time for the unknown property (ϕ). This is called Alterative direction implicit method due to the fact that for odd steps to solve the equations, previous step iteration value which are available are used for the present step as the known value at points 'w' and 'e' and the ϕ value for point p, n and s are unknown value so solving one dimensional problem with TDMA method which is discussed in Appendix C, we get the unknown value of ϕ at 'p', 'n' and 's' points. Similarly, for even steps to convert the equation into one dimensional, previous step ϕ values at 'n', 's' and 'p' are used and ϕ values at w,p and s which are unknown at given step are found by solving one-dimensional problems with the help of TDMA method.

Another alternating direction method is discussed by Yarenko (ref. 7) which is called method of fractional steps.

Step 1,3 . . . (odd)

$$\frac{\partial^2 \phi}{\partial z^2} = R(I,J) \frac{\partial \phi}{\partial x}$$

Steps 2, 4 . . . (even)

$$\frac{\partial^2 \phi}{\partial y^2} = R(I,J) \frac{\partial \phi}{\partial x}$$

But this method cannot be used for the problem concerning developing nature of ' ϕ ' in 'y' and 'z' direction and also in 'x' direction. This method can be used for solving fully developed velocity profile or fully developed temperature profile.

APPENDIX C: TRIDIAGONAL MATRIX ALGORITHM

This method is used to solve one-dimensional (Patankar, ref. 3) discretization equations. This is also called Gaussian elimination method. The designation of TDMA refers to the fact that when the matrix of the coefficients of these equations is written, all the non-zero coefficients align themselves along three diagonals of the matrix.

If we do note equations in general,

$$B_i \phi_i = C_i \phi_{i+1} + A_i \phi_{i-1} + D_i \quad (C1)$$

for $i = 1, 2, 3, \dots$. Thus the quantity ' ϕ_i ' is related to the neighboring ' ϕ ' quantities ϕ_{i+1} and ϕ_{i-1} . To account for the special form of the boundary point equations, let us set

$$A_1 = 0 \text{ and } C_N = 0 \quad (C2)$$

so that the ϕ_0 and ϕ_{n+1} will not have any meaningful role to play. These conditions imply that ' ϕ_1 ' is known in terms of ' ϕ_2 '. The equation for $i=2$ is a relation between ϕ_1 , ϕ_2 , and ϕ_3 . Since ϕ_1 can be expressed in terms of ϕ_2 , ϕ_2 can be expressed in terms of ϕ_3 . This process of substitution can be continued until ϕ_n is expressed in terms of ϕ_{n+1} . But because (ϕ_{n+1}) has no meaningful existence, we actually obtain the numerical value of ' ϕ_n ' at this stage. This enables us to begin the 'back substitution' process in which ' ϕ_{n-1} ' is obtained from ϕ_n , ϕ_{n-2} from ϕ_{n-1} , ϕ_2 from ϕ_3 and ϕ_1 from

' ϕ_2 .' This is called TDNA. Let us describe forward substitution process as follows:

$$\phi_i = P_i \phi_{i+1} + Q_i \quad \phi_{i-1} = P_{i-1} \phi_i + Q_{i-1} \quad (C.2.a)$$

$$B_i \phi_i = C_i \phi_{i+1} + C_i (P_{i-1} \phi_i + Q_{i-1}) + D_i$$

$$\text{where } P_i = \frac{C_i}{B_i - A_i P_{i-1}}, \quad Q_i = \frac{D_i + A_i Q_{i-1}}{B_i - A_i P_{i-1}} \quad (C.3)$$

for $i=1$,

$$P_i = \frac{C_i}{B_i} \quad \text{and} \quad Q_i = \frac{D_i}{B_i} \quad (C.4)$$

At the other end of P_i, Q_i sequence, we note that $C_n=0$ so $P_n = 0$.

So we can write

$$\phi_n = Q_n$$

SUMMARY OF TDNA

- (1) Calculate P_i and Q_i from equation (C.4)
- (2) Use the recurrence relations (C.3) to obtain P_i and Q_i for $i=2,3,\dots,n$
- (3) Set $\phi_n = Q_n$
- (4) Use equation

$$\phi_{i-1} = P_{i-1} \phi_i + Q_{i-1}$$

for $i=n-1, n-2, \dots, 3,2,1$ to obtain $\phi_{n-1}, \phi_{n-2}, \dots$

ϕ_3, ϕ_2, ϕ_1 .

This technique is very powerful means to solve one dimensional equations and it requires computer storage and computer time proportional only to 'N'.

APPENDIX D: PROGRAM 'HEAT'

```

DIMENSION U(50,5,12),A(50,5,12)
CALL SRCH$$ (2,'OUTPUT',6,1,N1,N2)
DO 10 K=1,50
DO 11 J=1,11
11  U(K,1,J)=0.0
DO 12 I=1,4
12  U(K,I,1)=0.0
10  CONTINUE
DO 13 J=1,11
DO 14 I=1,4
    U(1,I,J)=0.0
14  CONTINUE
13  CONTINUE
WRITE(5,30)
30  FORMAT('      K      I      J      U')
DO 15 K=1,49
DO 16 I=2,4
    U(K,I,12)=U(K,I,10)
DO 17 J=2,11
35  FORMAT(I3,5X,I3,5X,I3)
    U(K,5,J)=U(K,3,J)
    A(K,I,J)=U(K+1,I-1,J)+U(K,I+1,J)+U(K,I,J+1)+U(K+1,I,J-1)+0.
$1111
    U(K+1,I,J)=-00.185*U(K,I,J)+1.185*A(K,I,J)/4.0
WRITE(5,50) K,I,J,U(K+1,I,J)
50  FORMAT(I3,5X,I3,5X,I3,5X,E15.6)
17  CONTINUE
16  CONTINUE
15  CONTINUE
    CALL SRCH$$ (4,'OUTPUT',6,1,N1,N2)
CALL EXIT
END

```

APPENDIX E: CONVECTION PROGRAM

```

PROGRAM THERMAL(INPUT,OUTPUT,TAPE2=INPUT,TAPE3=OUTPUT)
COMMON A(7,21,26),8(7,21,26),C(7,21,26),D(7,21,26),T(7,21,26),R(
$7,21),J1
READ(2,*) ((R(I,J),J=1,11),I=1,4)
DO 5 J=1,11
DO 10 I=1,4
10 R(8-I,J)=R(I,J)
DO 15 I=1,7
15 R(I,22-J)=R(I,J)
5 CONTINUE
WRITE(3,78) ((I,J,R(I,J),I=1,7),J=1,21)
78 FORMAT(212,E15.6)
DO 20 I=1,7
DO 25 J=1,21
25 T(I,J,1)=23.0
20 CONTINUE
WRITE(3,30)
30 FORMAT(20X, * CONVECTION PROGRAM *)
J1=1
100 J1=J1+1
CALL EVEN
CALL TDMAEV
CALL PRINTT
IF(J1.EQ.26)GOTO 110
J1=J1+1
CALL ODD
CALL TDMAODD
CALL PRINTT
IF(J1.LT.26)GOTO 100
110 STOP
END

```

```

SUBROUTINE EVEN
COMMON A(7,21,26),B(7,21,26),C(7,21,26),D(7,21,26),T(7,21,
$26),R(7,21),J1
DO 45 I=2,5
DO 50 J=1,21
B(I,J,J1)=R(I,J)+2.0
A(I,J,J1)=-1.0
C(I,J,J1)=-1.0
50 CONTINUE
45 CONTINUE
DO 33 J=1,21
B(6,J,J1)=R(6,J)+2.0-2.0/(R(7,J)+2.0)
B(1,J,J1)=R(1,J)+2.0
A(1,J,J1)=0.0
C(6,J,J1)=0.0
C(1,J,J1)=-2.0
33 A(6,J,J1)=-1.0
DO 36 I=1,7
DO 37 J=2,20
37 D(I,J,J1)=T(I,J-1,J1-1)+T(I,J+1,J1-1)+(R(I,J)-2.0)*T(I,J,J
$1-1)
36 D(I,1,J1)=2.0*T(I,2,J1-1)+R(I,1)-2.0)*T(I,1,J1-1)
D(I,21,J1)=2.*T(I,20,J1-1)+(R(I,21)-2.0)*T(I,21,J1-1)
DO 48 J=1,21
48 D(6,J,J1)=D(6,J,J1)+(D(7,J,J1)+382.55)/(R(7,J)+2.0)
RETURN
END

```

```

SUBROUTINE TDMAEV
COMMON A(7,21,26),B(7,21,26),C(7,21,26),D(7,21,26),T(7,21,
$26),R(7,21),J1
DO 23 J=1,21
C(1,J,J1)=C(1,J,J1)/B(1,J,J1)
D(1,J,J1)=D(1,J,J1)/B(1,J,J1)
DO 3 I=2,6
E=1./(B(I,J,J1)-A(I,J,J1)*C(I-1,J,J1))
D(I,J,J1)=E*(D(I,J,J1)-A(I,J,J1)*D(I-1,J,J1))
3 C(I,J,J1)=E*C(I,J,J1)
T(6,J,J1)=D(6,J,J1)
DO 4 I=2,6
MI=7-I
4 T(MI,J,J1)=D(MI,J,J1)-C(MI,J,J1)*T(MI+1,J,J1)
T(7,J,J1)=(2.*T(6,J,J1)+382.55+D(7,J,J1))/(R(7,J)+2.0)
23 CONTINUE
RETURN
END

```

```
      SUBROUTINE PRINTT
      COMMON A(7,21,26),B(7,21,26),C(7,21,26),D(7,21,26),T(7,21,
$26),R(7,21),J1
      WRITE(3,11)J1
11      FORMAT(2X,2HK=,I2)
      DO 21 I=1,7
      WRITE(3,12)I
12      FORMAT(2X,2HM=,I2)
      DO 13 J=1,21,6
      WRITE(3,14)T(I,J,J1),T(I,J+1,J1),T(I,J+2,J1),T(I,J+3,J1),T
$(I,J+4,J1),T(I,J+5,J1)
14      FORMAT(5X,6E15.7)
13      CONTINUE
21      CONTINUE
      RETURN
      END
```

```

SUBROUTINE ODD
COMMON A(7,21,26),B(7,21,26),C(7,21,26),D(7,21,26),T(7,21,
$26),R(7,21),J1
DO 7 I=1,7
DO 8 J=2,19
B(I,J,J1)=R(I,J)+2.0
A(I,J,J1)=-1.0
C(I,J,J1)=-1.0
8 CONTINUE
B(I,1,J1)=R(I,1)+2.0
B(I,20,J1)=R(I,20)+2.0-2.0/(R(I,21)+2.0)
A(I,20,J1)=-1.0
A(I,1,J1)=-0.0
C(I,1,J1)=-2.0
7 C(I,20,J1)=0.0
DO 17 J=1,21
DO 9 I=2,6
9 D(I,J,J1)=T(I-1,J,J1-1)+T(I+1,J,J1-1)+(R(I,J)-2.0)*T(I,J,J1-1)
D(1,J,J1)=2.*T(2,J,J1-1)+(R(1,J)-2.)*T(1,J,J1-1)
17 D(7,J,J1)=2.*T(6,J,J1-1)+(R(7,J)-2.0)*T(7,J,J1-1)+382.55
DO 11 I=1,7
11 D(I,20,J1)=D(I,20,J1)+D(I,21,J1)/(R(I,21)+2.)
RETURN
END

```



```

SUBROUTINE TDMAODD
COMMON A(7,21,26),B(7,21,26),C(7,21,26),D(7,21,26),T(7,21,
$26),R(7,21),J1
DO 65 I=1,7
C(I,1,J1)=C(I,1,J1)/B(I,1,J1)
D(I,1,J1)=D(I,1,J1)/B(I,1,J1)
DO 66 J=2,20
E=1.0/(B(I,J,J1)-A(I,J,J1)*C(I,J-1,J1))
C(I,J,J1)=E*C(I,J,J1)
66 D(I,J,J1)=E*(D(I,J,J1)-A(I,J,J1)*D(I,J-1,J1))
T(I,20,J1)=D(I,20,J1)
DO 67 J=2,20
NJ=21 -J
67 T(I,NJ,J1)=D(I,NJ,J1)-C(I,NJ,J1)*T(I,NJ+1,J1)
T(I,21,J1)=(2.*T(I,20,J1)+D(I,21,J1))/(R(I,21)+2.0)
65 CONTINUE
RETURN
END

```

APPENDIX F: NON-DIMENSIONALIZATION OF MOMENTUM EQUATION FOR FULLY DEVELOPED FLOW

We are concerned with the solution of the convection problem through a rectangular duct having dimensions stated in the previous chapter. The flow through the rectangular duct is partially developing hydrodynamically and partially developed after a certain length of the tube. These aspects have been discussed in the previous chapter. We are interested in examining the thermal conditions on the quartz window heater of the convection cryomicroscope system. In the present study, the actual complex system has been simplified in order to develop a preliminary understanding of the problem. The window is situated at a distance beyond the critical length for the flow being fully developed so the flow in the region of our interest is hydrodynamically developed. In order to achieve the temperature profile along the surface of the heater window, we must determine the hydrodynamic characteristics of the channel flow velocity profile. After obtaining the velocity profile, we can use the hydrodynamic velocity information in the energy equation which will be discussed in the next chapter. To achieve the hydrodynamic solution, we begin by stating the Navier Stokes equations which are:

x direction:

$$u \frac{\partial u}{\partial x} + v \frac{\partial u}{\partial y} + w \frac{\partial u}{\partial z} = - \frac{1}{\rho} \frac{\partial p}{\partial x} + \nu \left(\frac{\partial^2 u}{\partial x^2} + \frac{\partial^2 u}{\partial y^2} + \frac{\partial^2 u}{\partial z^2} \right) \quad (F1)$$

y direction:

$$u \frac{\partial v}{\partial x} + v \frac{\partial v}{\partial y} + w \frac{\partial v}{\partial z} = - \frac{1}{\rho} \frac{\partial p}{\partial y} + \nu \left(\frac{\partial^2 v}{\partial x^2} + \frac{\partial^2 v}{\partial y^2} + \frac{\partial^2 v}{\partial z^2} \right) \quad (F2)$$

z direction:

$$u \frac{\partial w}{\partial x} + v \frac{\partial w}{\partial y} + w \frac{\partial w}{\partial z} = - \frac{1}{\rho} \frac{\partial p}{\partial z} + \nu \left(\frac{\partial^2 w}{\partial x^2} + \frac{\partial^2 w}{\partial y^2} + \frac{\partial^2 w}{\partial z^2} \right) \quad (F3)$$

In the above equations, we have made the following assumptions:

- (i) the flow is steady ($\frac{\partial \phi}{\partial t} = 0$ where ϕ = velocity in given direction)
- (ii) three dimensional flow
- (iii) incompressible flow ($\rho = \text{const.}$)
- (iv) constant property flow

We are interested in finding the fully developed velocity profile, so

$$v = 0, w = 0 \text{ and } \frac{\partial u}{\partial x} = 0 \text{ in each direction}$$

in (F1, F2, F3)

So, x dirⁿ momentum equation becomes

$$\frac{\partial^2 u}{\partial y^2} + \frac{\partial^2 u}{\partial z^2} = \frac{1}{\mu} \frac{\partial p}{\partial x} \quad (F4)$$

$$\text{x dir}^3: \quad \frac{\partial p}{\partial y} = 0 \quad (F5)$$

$$\text{z dir}^3: \quad \frac{\partial p}{\partial z} = 0 \quad (F6)$$

So from equations F4, F5 and F6, we get

$$\frac{dp}{dx} = \text{constant} \quad (U = f(y, z) \text{ but } u \neq f(x))$$

So $p = f(x)$ only.

Rewriting the equation (4) we get

$$\frac{\partial^2 U}{\partial y^2} + \frac{\partial^2 U}{\partial z^2} = \frac{1}{\mu} \frac{dp}{dx} \quad (F7)$$

The x direction momentum equation is non-dimensionalized by defining $U^+ = \frac{U}{U^+}$ where

$$U^* = \frac{-1}{\mu} \frac{dp}{dx} a^2 \left(\frac{1}{N/M^2} \times \frac{n}{N/M^3} \times m^2 \right) = (m/sec)$$

$$y^+ = \frac{y}{a} \left(\frac{m}{m} \right)$$

$$z^+ = \frac{z}{a} \left(\frac{m}{m} \right)$$

where a = width of the rectangular cross section as shown in Figure 3. The x direction equation is non-dimensionalized in order to generalize the solution which we obtain for various aspect ratios and various pressure drop magnitudes. The non-dimensionalized solution can be used to get various information about the effects of pressure drops and dimensions of the duct on the velocity magnitude at given locations in the duct.

So converting the coordinate system Y and Z into non-dimensionalized coordinates y^+ and z^+ , the width of the duct equals unity (the length of rectangular duct equals (b/a)). Now converting equation F7 into a non-dimensionalized form,

$$\left(\frac{U^*}{a^2} \right) \frac{\partial^2 U^+}{\partial y^{+2}} + \left(\frac{U^*}{a^2} \right) \frac{\partial^2 U^+}{\partial z^{+2}} = \frac{1}{\mu} \frac{dp}{dx}$$

$$\frac{\partial^2 U^+}{\partial y^{+2}} + \frac{\partial^2 U^+}{\partial y^{+2}} = \frac{1}{\mu} \frac{dp}{U^*} \left(\frac{a^2}{U^*} \right) \quad (F8)$$

Substituting the value of $U^* = -\frac{1}{\mu} \frac{dp}{dx} a^2$ on the right hand side of the above equation (8), we get

$$\frac{\partial^2 U^+}{\partial y^{+2}} + \frac{\partial^2 U^+}{\partial z^{+2}} = -1 \quad (F9)$$

REFERENCES

REFERENCES

- (1) Diller, K.R., and Cravalho, E.G., "A Cryomicroscope for the study of Freezing and Thawing Processes in Biological Cells," *Cryobiology*, 7, (1970):191.
- (2) Hrycaj, Thomas, "The Effects of Freezing on the Micro-circulation of the Hamster Cheek Pouch" (M.S. thesis, Massachusetts Institute of Technology, 1975).
- (3) Patankar, Suhas V., *Numerical Heat Transfer and Fluid Flow*, McGraw-Hill, New York, 1980.
- (4) Smith, G.D., "Numerical Solution of Partial Differential Equations," Finite Difference Method, 2nd ed.
- (5) Hornbeck, Robert W., "Numerical Marching Techniques for Fluid Flows with Heat Transfer" National Aeronautics and Space Administration, NASA SP-297, (1973):241.
- (6) Roache, Patric J., Computational Fluid Dynamics, Hermosa Publishers, Albuquergue, N.M., 1972.
- (7) Yonenko, Springerkerlag; Shoverly, M.M., and Gaane, R. R., Journal of Comp. Physics, 23, (1977):242.
- (8) Kays and Crawford, Convective Heat and Mass Transfer, 2nd Edition McGraw-Hill, 1980.
- (9) Shah, R.K., and London, A.L., "Laminar Flow Forced Convection in Ducts," in Advances in Heat Transfer, Academic Press, New York 1978.
- (10) Knudsen, James, and Katz, Fluid Dynamics and Heat Transfer, McGraw-Hill, New York, 1958.
- (11) Roshsenow, Warren M., and Choi, Henry, Heat, Mass and Momentum Transfer, Prentice-Hall; Englewood Cliffs, N.J.:1961.
- (12) Hornbeck, Robert, "Marching Solutions for Fluid Flows with Heat Transfer" (NASA Research Center), (1973), p.241.
- (13) Preingerova, Vera, "Laminar Entry Length Heat Transfer in Ducts of Rectangular Cross Section with Boundary Conditions of the Second Kind," in Heat Transfer Source Book (Minsk: Fifth All Union Conference, 1976), p. 74.

- (14) Preingerova, Vera, and Allen, P.H., "Laminar Flow Entry Length Heat Transfer with Varying Physical Properties in Simple and Complex Duct Geometries" (paper presented at the Heat Transfer Conference, Tokyo, 1974) (NC 5-4).
- (15) Sastri, V.M., and Chandrapatla, Ashok, "Laminar Flow and Heat Transfer to a Non-Newtonian Fluid in an Entrance Region of a Square Duct with Presented Constant Axial Wall Heat Flux," in Numerical Heat Transfer, 1, (1979):243.
- (16) Cess and Shaffer, "Heat Transfer to Laminar Flow Between Parallel Plates with Prescribed Wall Heat Flux," Applied Scientific Research Journal, A8, (1959):339.
- (17) Montgomery, S.R., and Wibulsatas, P., "Laminar Flow Heat Transfer for Simultaneously Developing Velocity and Temperature Profiles in Ducts of Rectangular Cross Section," Applied Scientific Research Journal, 18, (1967):247.
- (18) Lenert, Louis W., Advanced Technical Mathematics, Merril, Columbus, Ohio, (1970):327.

MICHIGAN STATE UNIV. LIBRARIES



31293009962568